5-1-2015

Timing of erosional episodes in the Marble Canyon and Vermilion Cliffs region from apatite (U-Th)/He thermochronology

Nadine Lynne Warneke

Nadine L. Warneke
Candidate

Earth and Planetary Science
Department

This thesis is approved, and it is acceptable in quality and form for publication:

Approved by the Thesis Committee:

Dr. Karl Karlstrom , Chairperson

Dr. Laura Crossey

Dr. Shari Kelley

TIMING OF EROSIONAL EPISODES IN THE MARBLE CANYON AND VERMILION CLIFFS REGION FROM APATITE (U-TH)/HE THERMOCHRONOLOGY

by

NADINE L. WARNEKE

B.S., GEOSCIENCES, UNIVERSITY OF ARIZONA, 2012

THESIS

Submitted in Partial Fulfillment of the
Requirements for the Degree of

Master of Science
Earth and Planetary Sciences

The University of New Mexico
Albuquerque, New Mexico

May 2015

Acknowledgements

I would like to thank numerous individuals for their aid and contribution to this project. First and foremost, I would like to thank Dr. Karl Karlstrom for his help and guidance on my project, as well as for providing me with the opportunity to see my unbelievable field area, by way of rafting, numerous times throughout my time at UNM. I would also like to thank Dr. Shari Kelley for her invaluable help in preparing my samples and teaching me about the elusive world of apatite thermochronology. I am greatly appreciative of the help of my committee member, Dr. Laura Crossey, both in the field and back home in the department. I would also like to thank Dr. Jason Ricketts for his time, not only collecting samples on numerous occasions, but also for the countless hours of microscope aid and collaborative driving to get to the lab. Finally, I would like to thank Tyler Grambling for his support and encouragement throughout the thesis process.

TIMING OF EROSIONAL EPISODES IN THE MARBLE CANYON AND VERMILION CLIFFS REGION FROM APATITE (U-TH)/HE THERMOCHRONOLOGY

by

Nadine L. Warneke

B.S., Geoscience, University of Arizona, 2012
M.S., Earth and Planetary Sciences, University of New Mexico, 2015

ABSTRACT

The history of incision of the Marble Canyon segment of Grand Canyon, and the rate of retreat of the Vermilion Cliffs portion of the Grand Staircase, are examined using a synthesis of new and published low-temperature thermochronology datasets. I test models for a 50-70 Ma Marble Canyon and interpretations that postulate SW to NE progressive denudational stripping of the Colorado Plateau via cliff retreat. The main goal is to evaluate the timing of carving of Marble Canyon. Thermal history models were generated using HeFTy for 14 samples that range in elevation from 940 m (river level) to 2052 m (top of the Vermilion Cliffs) to 2420 m (top of the Kaibab uplift). I find that samples from these different elevations record different components of a multi-stage cooling history for this region. Samples along the Colorado River in Marble Canyon show that rocks resided above 110 °C until 30 to 40 Ma and cooled to near-surface conditions between 25 and 6 Ma, with progressively younger cooling ages upstream. Hence this portion of the Colorado Plateau was covered with approximately 2 kilometers of Mesozoic rock until 30 Ma, precluding the presence of a 50-70 Ma paleocanyon. Intermediate elevation samples on the Kaibab rim of Marble Canyon show rapid 30-15 Ma cooling due to regional denudation as the Cretaceous section was eroded, but the pattern of cooling reflects carving of a 25-15 Ma paleocanyon across the Kaibab uplift, rather than a simple SW to NE cliff retreat. Post 10 Ma cooling along the river in Marble Canyon, further denudation of the top of the Kaibab uplift, and in

the headwaters of Kanab Creek, indicate that the modern Grand Staircase cliff retreat accelerated in the last ca. 10 Ma, but with geometry initiated in the last 25 Ma due to base level caused by the 25-15 Ma paleocanyon. Major findings are that: 1) Marble Canyon was carved quickly in the last ~10 Ma. 2) An early stage of cooling seen in many samples is attributed to cliff retreat initiated by carving of East Kaibab paleocanyon 25-15 Ma; 3) Formation of the Grand Staircase accelerated in the last ca. 10 Ma once the Colorado River was integrated through Marble Canyon area in the last 6 Ma. 4) Current interpretations for episodic incision 70-50, 25-15, and post- 10 Ma seem most consistent with a combination and interplay between vertical incision of paleocanyons that then triggers cliff retreat of rims.

TABLE OF CONTENTS

LIST OF FIGURES

LIST OF TABLES

INTRODUCTION

The Grand Canyon region provides one of the world's iconic landscapes shaped by plateau uplift and erosional denudation. At the end of the Cretaceous, much of the southwestern Colorado Plateau was covered by 2-3 kilometers of Paleozoic and Mesozoic sedimentary rock now seen in the stair-stepped cliffs of the Grand Staircase (Dutton, 1882) north of Grand Canyon (Doelling et al., 2000; Flowers et al., 2008; Lee et al., 2013; Dumitru et al., 1994). This region has now been eroded and sculpted into the Grand Canyon, the East Kaibab Uplift, and the sequence of cliffs, known as the Grand Staircase (Fig. 1, map). Much work has been done to study the evolution of the Grand Canyon (e.g. Young and Spamer, 2001) with recent studies focusing on data from low temperature thermochronology methods, which provide data on canyon incision and cliff retreat histories over tens-of-million-year timescales (Kelley et al., 2001; Flowers et al., 2007, 2008; Karlstrom et al., 2008; Lee et al., 2013; Karlstrom et al., 2014a) .

The debate about the age and formation of the Grand Canyon involves two end member hypotheses. The "old" canyon hypothesis (Wernicke, 2011; Flowers et al., 2008; Flowers and Farley, 2012) postulated that the Grand Canyon was carved in its present position and to near its modern depth by 80-50 Ma (Fig. 2). Flowers et al., (2008) used AHe ages to show staged denudation starting in the Mogollon Highlands southwest of the Grand Canyon region, and progressing north and east towards Lee's Ferry. The details of this model are shown in Figure 2C. As shown in cross section from the same paper, Flowers et al. (2008, their fig. 7C) proposed that a section of Marble Canyon was carved between 50 and 80 Ma and has been cutting deeper since then as the plateau around it continued denuding. Wernicke (2011) proposed two paleorivers, shown in Figures 2A&B as

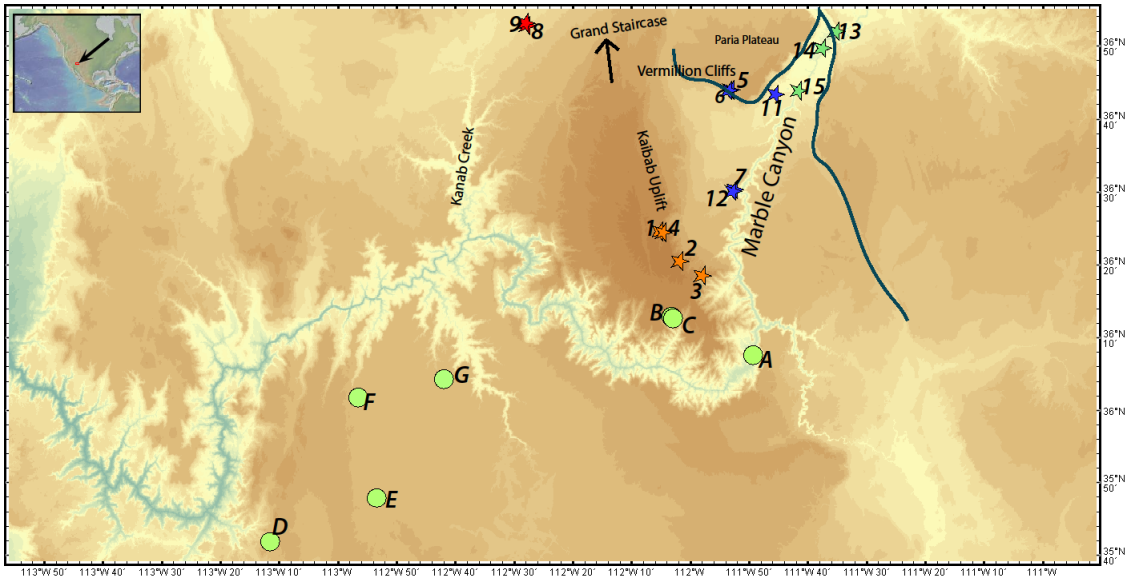

Figure 1. Map of key samples used in this study. Samples from this study are shown as blue stars (K11-VC-1790, K11-VC-2052, K12-SC1, K12-32-SOUTH4, K12-32-SOUTH7). Flowers et al., 2007 & 2008 are shown in orange stars (PGC-002, PGC-004, PGC-006 and PGC-011) and red stars (PGC-015 & PGC-016). Lee et al., 2013 samples are shown in green stars (01GC90, 01GC92, 01GC93). Samples not analyzed in this study, but mentioned in the text are shown in dark green circles for Lee et al., 2013.

the Arizona and California paleorivers. He posited that the California paleoriver carved the Grand Canyon from the west at 80 Ma following the entire course of the modern Grand Canyon. Then, by 55 Ma, Wernicke hypot sized a drainage reversal, with the Arizona paleoriver originating in the east and flowing west and Marble Canyon and Little Colorado River as tributaries. The combined rivers were proposed to have carved the modern Grand canyon to near-modern depths. In terms of overall plateau denudation, Flowers et al. (2008) showed three domains of AHe ages (using the minimum ages from samples) as shown in Fig. 2C. The southwestern domain, which included western Grand Canyon, has minimum AHe ages of 35-60 Ma that reflect cooling during uplift and erosion of the Mogollon highlands following Laramide deformation. The central domain, including eastern Grand Canyon, had 25-15 Ma minimum AHe ages, while the northern domain exhibited post-10 Ma minimum AHe ages. They proposed that denudation in the Grand Canyon region occurred in a 3-staged sweep (Flowers et al., 2008, p. 580) from southwest to northeast across the plateau from the Grand Wash cliffs to the Zion- Four Corners region.

"Young" Canyon models have been based mainly on the Muddy Creek constraint (Blackwelder, 1934; Longwell, 1936; 1946) that showed that the Colorado River did not follow its present path through Grand Wash cliffs until after 6 Ma. In contrast to both "old" and "young" canyon models, Lee et al. (2013) proposed an intermediate age for carving of part of modern Grand Canyon. These thermochronometric data suggested that eastern Grand Canyon was incised 25-15 Ma, but Marble Canyon was not formed until integration of the Colorado River 5 to 6 million years ago. Karlstrom et al. (2014) extended this model and hypothesized that "old", "intermediate", and "young" canyon segments became integrated into the present path of Grand Canyon at the same time that the Colorado River became

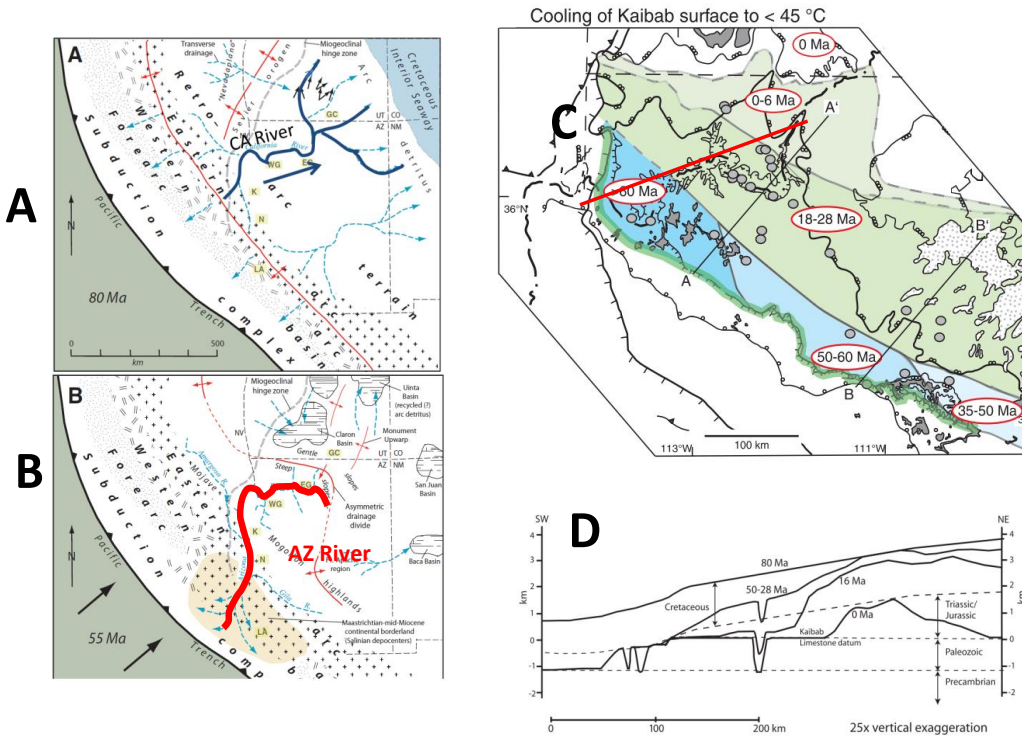

Figure 2. Figures from Flowers et al. (2008) and Wernicke (2011). (A) & (B) are two proposed paleorivers from Wernicke (2011) that shows the eastward flowing California river at 80 Ma and the westward flowing Arizona river at 55 Ma andpatterns of denudation across the plateau 60Ma to present, (C) is a map from Flowers et al. (2008) showing the time periods when the Kaibab surface cooled to below 45°C (D) proposed incisional history over time of drainages in the southwestern part of the Colorado Plateau from the A-A' line shown in (C).

integrated from the Colorado Plateau to the Gulf of California 5-6 Ma. In this "paleocanyon solution," Karlstrom et al. (2014a) suggested that each segment of Grand Canyon may have somewhat separate incision histories prior to integration of the Colorado River. Thus, one test of the "old" Grand Canyon hypotheses is to examine each segment; if any are "young" segments then the "old canyon" hypotheses must be modified. The present study is a test of this hypothesis with respect to Marble Canyon, the most upstream segment of Grand Canyon.

The goals of this study are to compile, model, and interpret all available thermochronologic data to examine the proposed mechanisms and timing for the formation of Marble Canyon. I use both new and published data and a combination of AFT and AHe data. These are modeled in HeFTy (Ketcham, 2005) using a uniform and defined set of geologic constraints for the models that are based on known stratigraphic thicknesses and orogenic events. The results are then interpreted in terms of the age for the carving of Marble Canyon and the initiation of cliff retreat that formed the Grand Staircase.

GEOLOGIC AND STRATIGRAPHIC BACKGROUND

The Great Denudation of Dutton (1882) involved the erosion of 2-3 km of mainly Mesozoic strata from most of the southern and central Colorado Plateau. This erosion involved both vertical river incision that produced deep canyons like Grand Canyon, and lateral cliff retreat, which produced a series of stepped cliffs between Grand Canyon and Bryce Canyon National Parks called the Grand Staircase (Ranney, 2014).

Vertical incision rate studies have been conducted in the Marble Canyon area over the last decade. The most important location for direct estimates of Quaternary incision rates is located near the confluence with the Little Colorado River (Fig. 1). Terraces of different heights along the mainstem in this region are cemented by travertine and constrain late

Quaternary incision rates to be semi-steady at 160 m/Ma for the last 600 ka (Karlstrom et al., 2007; Pederson, 2008; Pederson et al., 2013; Crow et al., 2014). U-Pb dated speleothems from side canyons have also been used for incision estimates using an assumption that mammilaries on the roof of caves reflect the time of downward movement of the water table through the cave as the canyon and side canyons incised. Speleothem data from South Canyon suggest semi-steady incision of Marble Canyon at a rate of 236 m/Ma over the last 4 Ma, with somewhat slower rates post-600 ka (Polyak et al., 2008; Crow et al., 2014). This rate would be capable of carving the entire 1 km depth of Marble Canyon (near the LCR confluence) in 4 Ma.

Stratigraphic data for the Lees Ferry region are summarized in Fig. 3A. This figure is highly generalized but is aimed at showing the main packages at a scale that the thermochronology would reflect. Basement rocks are not exposed in Marble Canyon, but appear just west of the confluence with the Little Colorado River. Basement is overlain by ~1 km of Paleozoic rock-consisting of relatively resistant carbonates, sandstones, and shales. The top of this sequence is the Kaibab Limestone, which underlies the stripped surface that forms the rim of Marble Canyon. Triassic and Jurassic sections are dominated by relatively erodible sandstones and shales and are also ~1 km thick. These sediments have retreated from the rim of Marble Canyon but are present in the Vermilion cliffs just to the north, forming the first step of the Grand Staircase (Fig. 1). The Cretaceous section, composed of non-resistant sandstones and shales of the Cretaceous Western Interior Seaway, has been removed from the area of Figure 1, but 1-2 km of Cretaceous strata were initially deposited across the region and are preserved in the Grand Staircase region to the north near Zion and Bryce canyons, and in the Black Mesa region east of Grand Canyon. Thus the total thickness

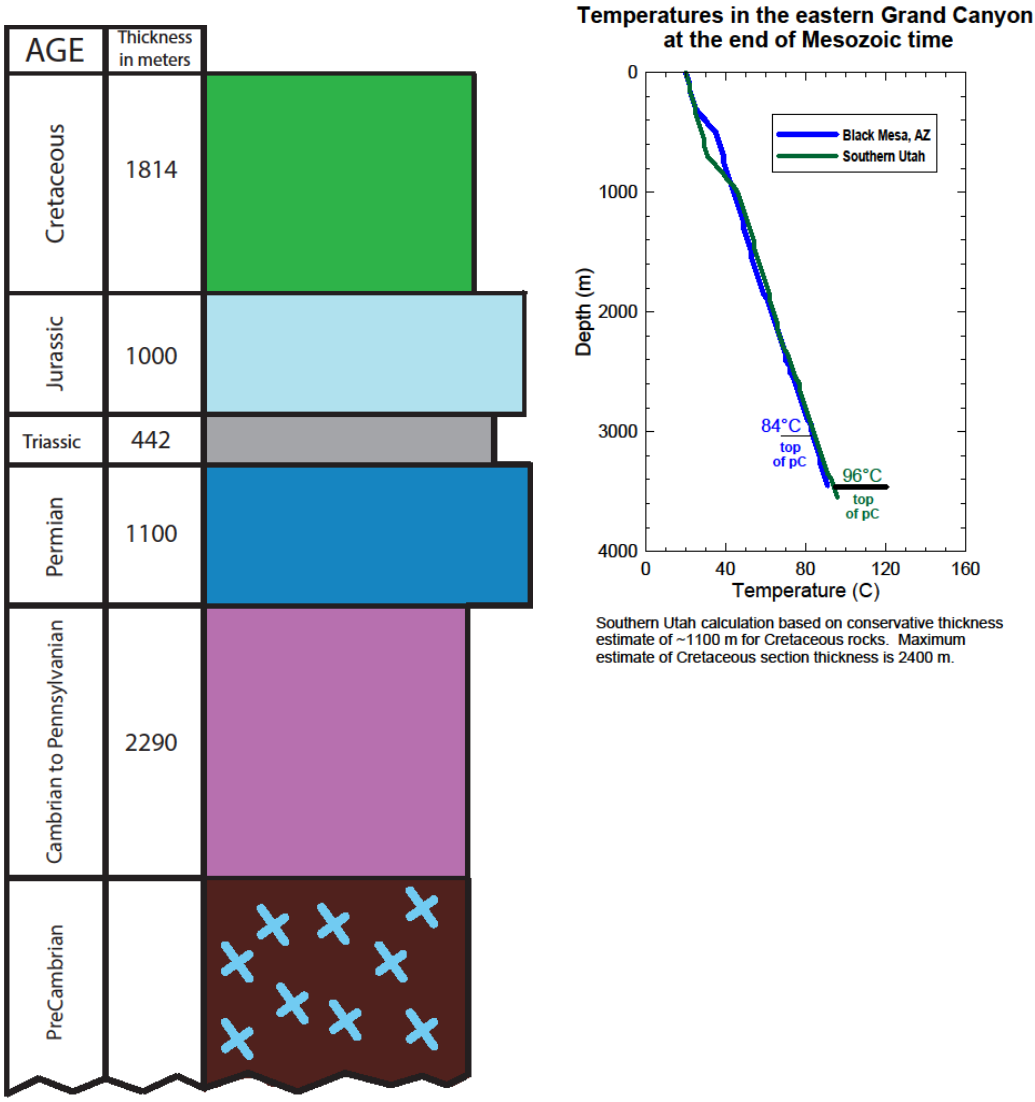

Figure 3A. A generalized stratagraphic section of the Cambrian to Cretaceous strata. Thicknesses are estimated from Doelling et al. (2000). B. Calculated geothermal gradients in the eastern Grand Canyon at the end of Mesozoic time based on thickness of rock in the Cretaceous, an estimated background heat flow of 63 mW/m^2 and a surface temperature of 20°C (Kelley, unpublished).

of sedimentary rock that was deposited in the region reached about 3-4 km by ~ 80 Ma. The region was still at sea level at this time.

Fig. 3B shows the calculated (immediately pre-Laramide) isotherm structure inferred from estimated heat flow values and thermal conductivity structure of the sedimentary section. This suggests that 50ºC and 100°C paleo-isotherms (at 80 Ma) were located near the top of the Paleozoic section, and near the top of the Precambrian basement, respectively. Thus, most basement rocks at 80 Ma would have been above the ~ 110° closure temperature for the AFT system and hence zero age at 80 Ma, and most Paleozoic rocks would have been above the 40-90ºC closure temperature of the AHe system and hence zero age at 80 Ma. The slope of this line provides an estimated geothermal gradient of 20 ºC/km, which is the geothermal gradient I use throughout this paper to convert temperature to depth. The gradient extrapolates to a surface temperature of 20 ºC and provides an average surface temperature for temperature-to-depth conversions. These values are slightly lower than the 25°C/km and 25°C surface temperature used by Flowers and Farley (2012), and both provide potential estimates for depth of erosion at different times across the region (see discussion in Karlstrom et al., 2014, supplementary materials).

Figure 4, taken from Dickinson (2012), shows the distribution of strata in the Grand Staircase. Important features for this study include Kaibab rim of Marble Canyon, the Paria Plateau and Vermilion Cliffs near Lees Ferry, the Kaibab uplift, the Triassic rocks at the head of Kanab Creek, and the Grand Staircase cliffs that extend from Grand Canyon to the Zion plateau.

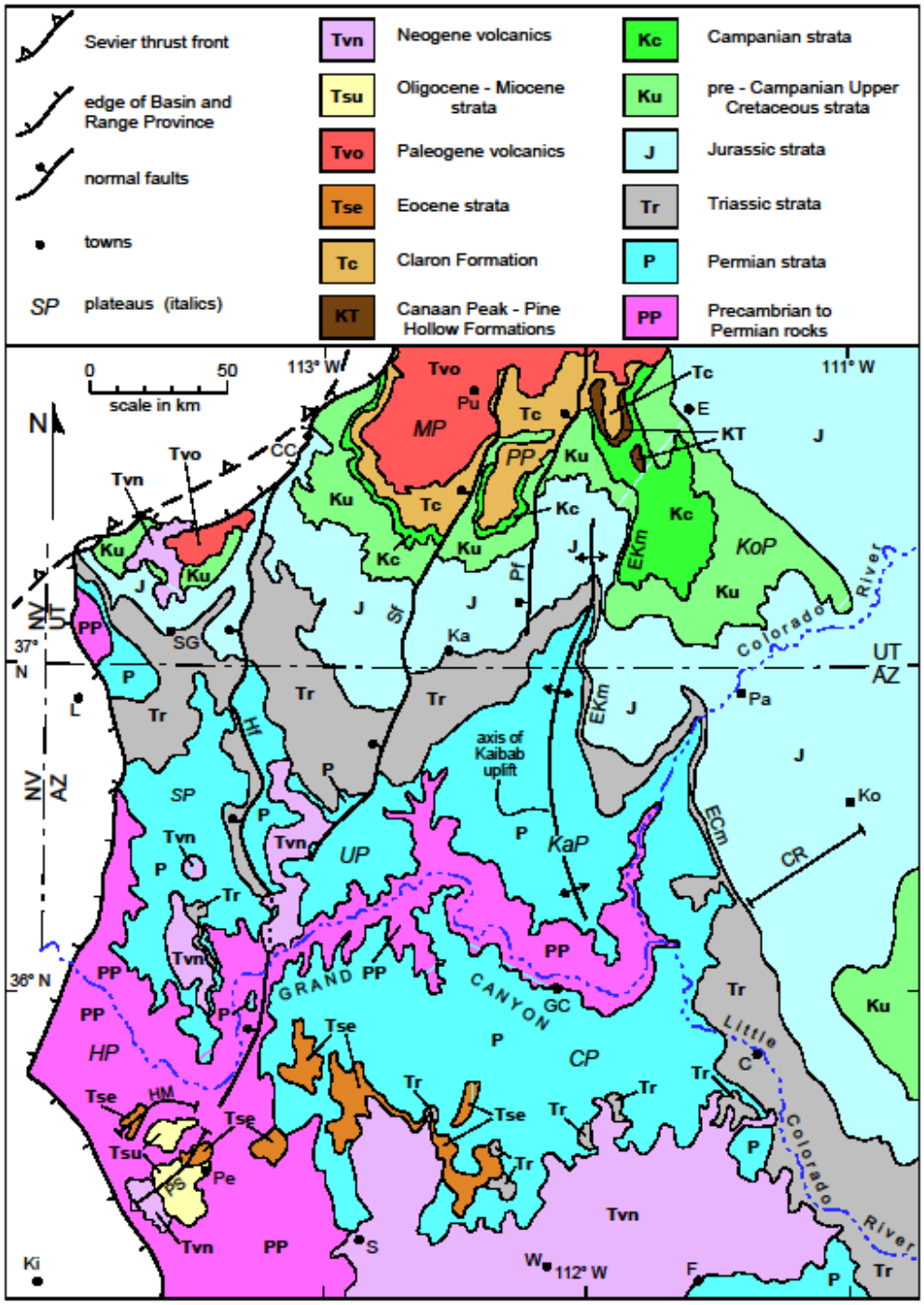

Figure 4. Generalized geologic map of the southwestern Colorado Plateau from Dickinson (2012).

METHODS

AHe Thermochronology

The use of the apatite (U/Th-He) system as a low temperature thermochronometer is well established and has been applied to many studies in geology, tectonics and geomorphology (e.g. Ehlers and Farley, 2003; Farley, 2000; Farley and Stockli, 2002; Stockli et al., 2000). The premise of the system is based on the alpha decay of ^{235}U, ^{238}U and ^{232}Th to produce radiogenic helium. In apatite crystals, helium is not retained within the crystal lattice above temperatures of around 50-90°C, depending on apatite composition, and is not fully retained in the grain until it cools to temperatures less than 40°C. Closure temperatures vary from grain to grain, depending on grain size, cooling rate and effective uranium (eU), as defined by the equation eU=[U]+0.235[Th]. The effect of eU has been studied in apatite grains in the Grand Canyon by Flowers et al. (2008) and effects of eU in modeled time-temperature paths is considered later in this paper. Other considerations include radiation damage and lattice damage, ideas set forth by Shuster et al. (2006), Flowers et al. (2009), Shuster and Farley (2009) and Fox and Shuster (2014).

The process for determining AHe dates involves multiple iterations between sampling and the lab. Rocks must be crushed and separated by mineral density and magnetic properties, which was done by at Zirchron LLC in Tucson, AZ. Samples were then returned and examined under a microscope at New Mexico Institute of Mining and Technology, under the supervision of Shari Kelley. Grains are picked based on grain, size, shape, and lack of imperfections such as zoning, inclusions and breaks. Grains are then individually packed into small platinum tubes and sent to AHe facilities at the University of Colorado at Boulder and University of California, Berkley.

AFT Thermochronology

AFT dating uses the spontaneous fission of ^{238}U and its affects on the crystal lattice of apatite grains. The fission creates tracks in the crystal which can be counted and measured for length to determine the time when the apatite grain cooled between temperatures of ~60-110°C. At temperatures higher than this, tracks can be annealed through recrystallization. Track density and length data can help constrain the thermal evolution of samples at these higher temperatures and, therefore, at deeper burial depths than AHe thermochronology.

HeFTy Thermal History Modeling

Interpretation involved using data from the ICP-MS, grain size and uncorrected age of the grains. Inverse modeling was done using the software HeFTy, version 1.7.5 (Ketcham, 2005). To run thermal models in this program, the user inputs data for at least one grain; the model has the capability to include data for up to 7 grains at once. Input data for each grain can be either apatite (U-Th)/He, or apatite fission track, or both.

For modeling assumptions, a geothermal gradient near the end of the Laramide of approximately 20 ºC/km is assumed, based on Figure 3B. An approximation of 70-90 Ma for the beginning of the Laramide orogeny is taken from Kelley et al. (2001; also see Karlstrom et al., 2008; Wernicke, 2011; Flowers and Farley, 2012). However, maintenance of a constant geothermal gradient and surface temperature through the last 70 Ma is unlikely (Karlstrom et al., 2014b) so resolution of post-Laramide paleo-depth from modeled paleo-temperatures has considerable geologic uncertainty (Karlstrom et al., 2014, supplementary materials). The role of groundwater in influencing geothermal structure is ignored for present purposes, but hydrological studies show temperatures of ~ 20 ºC in the Redwall Limestone karst aquifer (Crossey et al., 2009) which may reset the "surface temperature" boundary

condition at this stratigraphic depth regardless of the average surface temperature at a given time. For this reason, and uncertain temperature-to-depth conversion assumptions, the HeFTy models are unlikely to provide meaningful constraints on temperatures less than 30-40°C (depths of 500-1000 km using 20ºC and 20ºC/km, or minimum depths of 200-600 m (based on 20-25ºC surface temperatures and 20-25ºC/km geothermal gradient assumptions) as rocks cooled toward the surface.

Constraint boxes imposed into HeFTy are valuable ways to integrate firm geologic knowledge into inverse modeling and thus both reduce modeling time and assure more geologically reasonable T-t models. Beginning parameters for time-temperature modeling were chosen based on existing detrital zircon data from each rock unit (Dickinson and Gehrels, 2003; Gehrels et al., 2011), with the assumption that a majority of the apatites grains in the rock unit crystallized from the same units that produced a majority of the zircon grains. About 80% of grains from Mesozoic sandstones are Precambrian so a broad constraint box of 150-250°C from 1.4 to 1.0 Ga was used. This is compatible with cooling of much of the region's basement rocks through ~200°C argon K-feldspar closure temperatures in the 1.4 to 1.0 Ga timeframe (Timmons et al., 2005). This constraint has the effect on thermal models of giving apatite grains hundreds of millions of years to acquire radiation damage as they cooled to surface temperatures by Cambrian time. This radiation damage in crystals can have an important effect on subsequent degree of annealing that took place during sediment burial prior to Laramide orogeny (Fox and Shuster, 2014). A depositional age constraint box was assigned based on the unit's stratigraphic age (Pennsylvanian to Jurassic; Table 1) such that all cooling paths are constrained to surface temperatures of 5- 25° C at the time of deposition of the sedimentary units.

A constraint box was also used for the pre-Laramide burial of samples. I selected a broad constraint of 40ºC to 140°C between 70 to 90 Ma. These temperature constraints were based on minimum and maximum burial depths of the samples, which could have ranged from 1 to 3 km depending on the original stratigraphic thickness in the region. There is some uncertainty regarding how much Cretaceous rock was deposited in the region. Preservation of ~ 1 km near Black Mesa provides a minimum estimate as the top of the section is not preserved (Nations et al., 2000) and Kaparowitz Plateau thickness of 2 km (Doelling, 2008) provides a maximum and probably more realistic burial thickness. 2-3 km of burial equates to 60-80°C based on assumed 20°C surface temperatures and 20°C/km geothermal gradients (75-100°C based on 25°C and 25°C/km). I could have used this smaller constraint box (60-100°C at 90-80 Ma). However, the broader 40-140°C constraint allows for a broader range in long term surface temperature (10-25°C) and geothermal gradient (15-25°C/km) assumptions, the effects of low thermal conductivities in blanketing Cretaceous shales, as well as the possibility of Lower Tertiary strata above the Cretaceous rocks (nearly 4 km of burial). This broader constraint box also has the advantage of allowing the thermochronologic data themselves to estimate the pre-Laramide depth of burial of samples. The final constraint box I used was a surface temperature box of 5-25°C at 0 Ma. Examples of all of these constraint boxes can be seen in Appendix A.

Sensitivity tests for the modeling are shown in Appendix A. This shows that the Precambrian basement constraint box makes little difference (compare A and B). However, use of the depositional constraint box was important (compare B and C), possibly because it allowed grains to build up a longer history of radiation damage and helium accumulation. Using just the Laramide constraint box (C; as was done by Lee et al. (2013; specific time and

temperature ranges for different regions are found on page 7 of their document), and Flowers et al (2008; they used a Laramide point of approximately 80 Ma and 80°C) produced slightly cooler post-Laramide temperatures and, more importantly, was unable to provide useful information about peak temperatures reached just prior to the Laramie orogeny. Modeling runs using one million random path attempts produced essentially the same T-t paths and ratio of good paths/path attempts (0.005) and acceptable paths/path attempts (0.028) as runs that were terminated after 100 good paths were generated.

When samples were run with multiple grains, a goodness of fit of 0.5 for good and 0.05 for acceptable paths was used. When running single grain models, a goodness of fit of 0.95 was used for both good and acceptable fits. "[T]he GOF value has an easily interpretable meaning that is analogous to the K-S test result, only I have reversed the "known" and "sample" entities. A value of 0.05 means that 5% of possible random samples from the distribution described by the data are further away from the measured age than the model age, and the expected value for a random sample taken from the data distribution is 0.5" (Ketcham, 2005).

Modeling efforts entered combinations of the single grain constraints for each sample, and any AFT data that are available. The Flowers samples had 6-12 grains analyses per sample, yet few of these samples produced acceptable or good paths with all of the grains entered (see Table 1). Instead, models generated with a subset of grains are used as my best constraints on T-t history of the samples. The width of the band of good fit paths generally has 10-20°C spread of uncertainty in most models, so HeFTy produces a weighted mean best fit path (smooth black line) and statistical best fit path (usually a more jagged black line). The mean path is calculated in HeFTy by weighting the fit of the path, which is a value

between 0 and 1.0, and calculating the mean path value for the whole time length of the modeled paths. These paths are thus considered most representative of the actual cooling path of the samples and I use them for comparisons of models.

In an effort to use more of the grain constraints, I also applied single grain HeFTy models to individual grains that could not be modeled in the successful multigrain runs. As shown in Appendix A, these allowed me to estimate a range of closure temperatures most likely to be represented by each grain based on its grain size and composition. These seem useful to show as comparison boxes and are invariably consistent with the successful multigrain models.

RESULTS

HeFTy models were run from all thermochronologic samples presently available. These include datasets from several published studies as shown in Table 1 (Flowers et al., 2007, 2008; Flowers and Farley, 2012; Lee et al., 2013). From Flowers et al. (2007 & 2008), I use (1).PGC-002, (2).PGC-004, (3).PGC-006, and (4).PGC-011 from near the top of the Kaibab uplift and (8).PGC-015 and (9).PGC-016 from west of the Kaibab Uplift near the headwaters of Kanab Creek. The number in the parenthesis are equivalent to the sample numbers on Figure 6 and Table 1. From Lee et al. (2013), I use a combination of AHe and apatite fission-track, (13). 01GC90, (14). 01GC92, (15).01GC93 from the river level. AHe samples from the North Rim of Grand Canyon on the Kaibab uplift were (B). GCNK1 & (C). GCNK4, AHe samples from the BM, Sage, SBF and Wate boreholes on the South Rim of Grand Canyon (D-G of Table 1).

New AHe samples were collected in vertical transects going up the Sand Crack of the Vermilion cliffs above highway 89A, one through Soap Creek, a side canyon to Marble

Supplementary Table 1: Key thermochronology samples discussed in text; Bold= new thermal models in this paper

Sample number (Fig 1) (depth in drill hole)	River Mile below Lee's Ferry	Elevation (m)	Latitude	Longitude	Rock type	AFT central age (Ma)	AFT mean track length (um)	AHe mean age (Ma)	AHe age range (Ma)	AHe mean eU (ppm)	AHe eU span (ppm)	#	references
1. PGC-004	**Kaibab uplift**	**2521**	**36.4104**	**-112.0869**	**Coconino**	**-**	**-**	**46.6**	**35-63**	**34**	**16.8-59**	**7**	**Flowers et al., 2007 & 2008**
2. PGC-011	**Kaibab uplift**	**2420**	**36.3421**	**-112.0306**	**Esplanade**	**-**	**-**	**49**	**26-67**	**46.9**	**16-162**	**7**	**Flowers et al., 2008**
3. PGC-006	**Kaibab uplift**	**2310**	**36.309**	**-111.9666**	**Esplanade**	**-**	**-**	**44**	**26-57**	**62.6**	**35-105**	**9**	**Flowers et al., 2008**
4. PGC-002	**Kaibab uplift**	**2292**	**36.4078**	**-112.077**	**Esplanade**	**-**	**-**	**46.4**	**19-69**	**77.3**	**25.6-115**	**7**	**Flowers et al., 2007 & 2008**
5. K11-VC-2052	**Vermillion Cliffs**	**2052**	**36.733308**	**-111.88488**	**?**	**-**	**-**	**73.4**	**73.4-73.4**	**21.9**	**21.9**	**1**	**this study**
6. K11-VC-1790	**Vermillion Cliffs**	**1790**	**36.731864**	**-111.89111**	**?**	**-**	**-**	**31.9**	**29.4-33.5**	**34.3**	**11.2-69.7**	**3**	**this study**
7. K12-32-SOUTH4	**32**	**1593**	**36.506012**	**-111.875**	**Kaibab**	**-**	**-**	**32.7**	**15.4-46.6**	**46.9**	**8.3-97.9**	**3**	**this study**
8. PGC-015	**Kanab Creek**	**1506**	**36.8798**	**-112.4639**	**Moenkopi**	**-**	**-**	**30**	**5-77**	**26.1**	**8.1-60.2**	**19**	**Flowers et al., 2007 & 2008**
9. PGC-016	**Kanab Creek**	**1491**	**36.8855**	**-112.4675**	**Moenkopi**	**-**	**-**	**45.5**	**13-104**	**35.4**	**13.7-94.1**	**13**	**Flowers et al., 2007 & 2008**
11. K12-SC1	**11**	**1254**	**36.723114**	**-111.75944**	**?**	**-**	**-**	**29.3**	**22.6-41.5**	**19.2**	**15.2-21.5**	**3**	**this study**
12. K12-32-SOUTH7	**32**	**1214**	**36.501996**	**-111.8793**	**Supai**	**-**	**-**	**22**	**20.2-23.8**	**57.4**	**43.2-71.5**	**2**	**this study**
13. 01GC90	**0**	**957**	**36.8666**	**-111.5872**	**Shinarump SS**	**30**	**12.7**	**10.6**	**5.6-19.2**	**48.6**	**19.0-105.5**	**4**	**Lee et al., 2013**
14. 01GC92	**3.6**	**945**	**36.8284**	**-111.6258**	**Toroweap SS**	**28.4**	**12.2**	**15.1**	**7.2-29.2**	**90.6**	**27.0-239.3**	**5**	**Lee et al., 2013**
15. 01GC93	**11.6**	**940**	**36.7312**	**-111.6931**	**Supai siltstone**	**39.4**	**-**	**18.5**	**16.6-20.3**	**91**	**54.7-158.8**	**3**	**Lee et al., 2013**
A. 01GC103	66.3	841	36.1271	-111.8223	Dox Sandstone	49	12.7	36.4	36.4-36.4	6	6	1	Lee et al., 2013
B. GCNK1	N Kaibab Rim	2391	36.2156	-112.0541	Toroweap SS	-	-	59.8	40.6-77.8	25	11-47	4	Lee et al., 2013
C. GCNK4	N Kaibab Rim	1999	36.2106	-112.0484	Supai siltstone	-	-	53	33.7-69.9	71	25-198	5	Lee et al., 2013
D. BM1	S Kaibab Rim	1619	35.6972	-113.1919	Toroweap SS	-	-	67.8	38.4-103	49	16-95	8	Lee et al., 2013
E. SBF2	S Kaibab Rim	1565	35.7985	-112.8901	Supai siltstone?	-	-	115	78.6-147.8	57	23-11	7	Lee et al., 2013
F. Wate1030	S Kaibab Rim	1496	36.0291	-112.9417	Supai siltstone?	-	-	47.7	36.9-64.4	29	22-32	4	Lee et al., 2013
G. Sage1	S Kaibab Rim	1564	36.0716	-112.6992	Supai siltstone?	-	-	62.9	31.1-86.8	44	15-74	6	Lee et al., 2013

Canyon at river mile 11 and the third at South Canyon, down the UPS route, near river mile 32 in Marble Canyon (Fig. 1). These had relatively poor apatite yield and these models are constrained by fewer grains. In all, 41 new samples were collected for this study. Twenty eight were sent for mineral separation and of those separated, five contained enough usable apatite to be sent for analysis at University of Colorado at Boulder with six more awaiting analysis at UC Berkley's geochronology lab. The usable samples from the Sand Crack came from elevations of 2052 meters and 1790 meters in the Navajo Sandstone. The only usable sample from Soap Creek came from the rim, in the Kaibab Formation, though previously reported data gives ages from the Esplanade Formation Colorado River level, within Marble Canyon. From South Canyon, river mile 32, I have one sample in the Kaibab Formation, at the rim of Marble Canyon, elevation 1593 and one sample from the Supai Group, approximately halfway down the cliff, at an elevation of 1214. Pending samples are along the river corridor at river miles 17, 20, 38.5, 49.9 and Nankoweap Mesa, mile 53 (Table 1).

The age-elevation distribution of all dated samples is shown in Fig. 5 with elevations that range from 841 m at river level in the Grand Canyon to 2521 m at the top of Kaibab uplift. This graph shows that apatites from individual samples give a wide range of AHe ages that span the entire 100-6 Ma Cenozoic cooling history of the region. This type of age spread may be expected from apatites from different elevations and with variable retentivity (and resulting variations in closure temperature) due to different amounts of radiation damage of apatite lattices (e.g. Flowers et al., 2007; Flowers, 2009). I infer from this pattern of diverse ages at all elevations, and from all stratigraphic levels (from the Precambrian to the Jurassic), as well as all structural positions from the top to the sides of the Kaibab uplift, that most

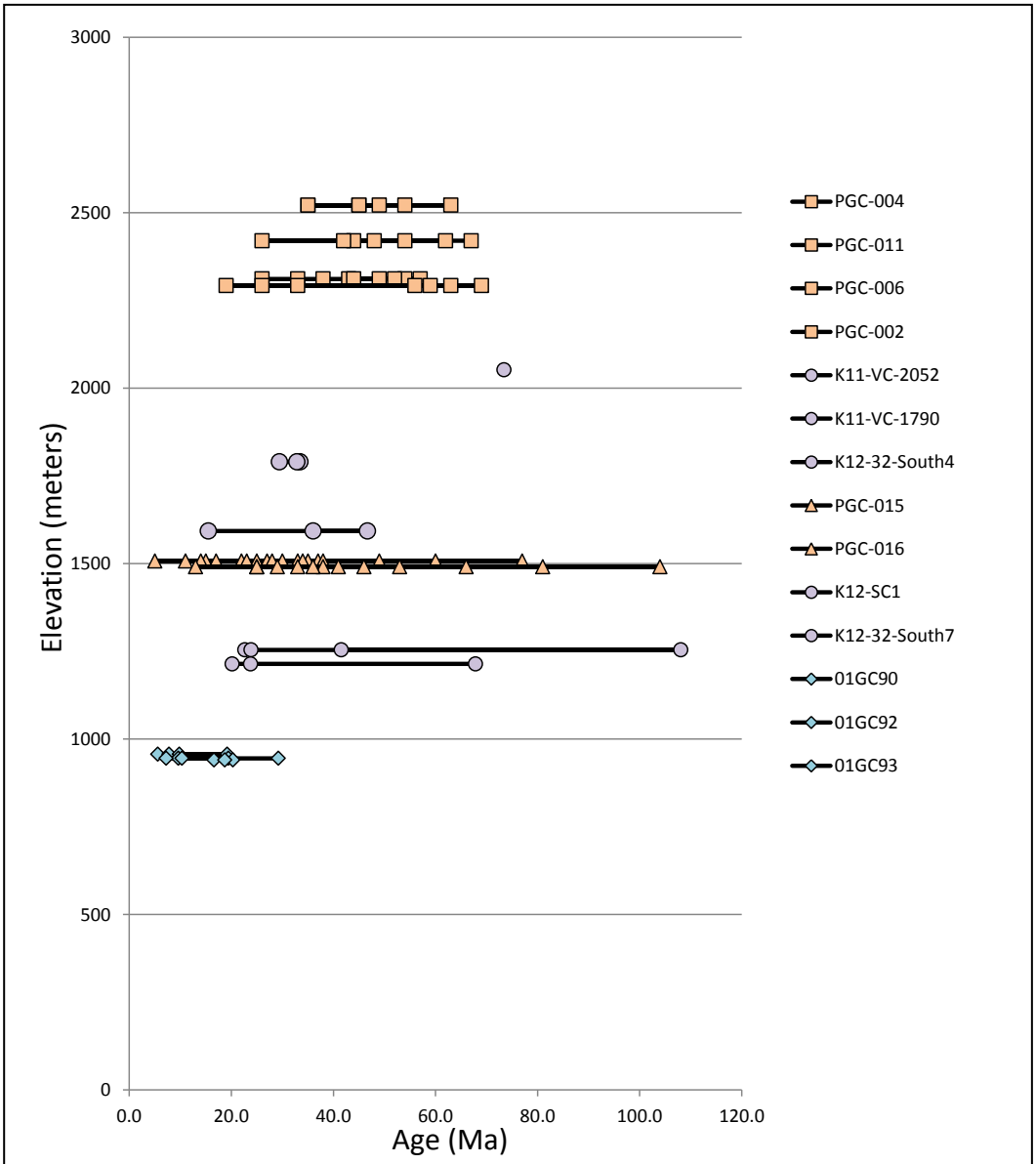

Figure 5. Age vs Elevation of Kaibab Uplift, Vermillion Cliffs & Marble Canyon. Colors and numbers correspond to sample numbers and row colors from Table 1.

samples resided in the partial retention zone (40-90°C) for AHe for much of post-Laramide time.

Full interpretation of this age-elevation graph requires addition of thermal models (below), but if the youngest grains of each sample is used as reflective of the lower closure temperature grains (e.g. as done by Flowers et al., 2008), there is a suggestion of kinks in age-elevation trends (Fig. 5) that imply that the data may contain evidence for a mid-Tertiary pulse of cooling/exhumation preserved at higher elevation and a ~10 Ma cooling at lower elevation. Such a multi-stage cooling history has been proposed for the Grand Canyon (Karlstrom et al., 2014a; Flowers et al., 2008) and Rocky Mountain regions (Karlstrom et al., 2012; Cather et al., 2012). Based on the Fig. 5 age-elevation graph, this multi-stage cooling history forms a testable hypothesis for this paper. The different slopes of the path envelopes of youngest grains may suggest more rapid cooling during the latter episode, which is also testable using the HeFTy models.

Thermal models and setting of samples will be discussed from highest to lowest elevations within several natural grouping: Kaibab uplift, North Rim of the Grand Canyon, Vermilion cliffs, Kanab drainage on North Rim, South Rim of the Grand Canyon, and Marble Canyon. An advantage of discussing samples in these grouping is that certain (obvious) geologic constraints must apply: 1) all detrital grains from the same sample must have had the same post-depositional heating then cooling path; 2) cooling paths from samples collected near the same elevation and from nearby locations must have similar cooling histories unless there are intervening faults.

Kaibab Uplift Samples

Four samples were collected from the Esplanade Sandstone (PGC- 002, PGC-006, PGC-011) and the overlying Coconino Sandstone (PGC-004) near the top of the Kaibab uplift (Flowers et al., 2008). The Coconino sample is approximately 100 m higher in the section than the other three, which would translate to a cooling path < 5°C cooler for the Coconino sample relative to the Esplanade samples (hence indistinguishable given thermochronologic resolution). A similar sample (GCNK1) was collected in the Toroweap sandstone nearer the North Rim of Grand Canyon (Fig. 1) and was modeled by Lee et al., (2013). All five of these samples are in close proximity, similar elevation, and similar stratigraphic level, and there are no major faults separating them. This indicates that all must have experienced similar cooling histories, which is a powerful geologic test of the HeFTy models. However, contrasting thermal history models were published for PGC-004 by Flowers et al. (2007) and Flowers et al. (2008) with the 2007 model closer to the Lee et al., (2013) model for North Rim sample GCNK1. My new HeFTy models for the four Kaibab Uplift samples are discussed below.

PGC-004 (Coconino Sandstone) had 7 grains analyzed (Flowers et al., 2008) but I was unable to get all grains to model together in HeFTy even after 1 million runs (Fig. 6). Successful models were run in HeFTy with 4 grains (Fig. 6), which show a good correlation between age and eU (triangles in Fig. 7). In agreement with the earlier model of Flowers et al. (2007) (but not Flowers and Farley 2013), my new model with 1 million paths yielded 5661 good paths (GOF = 0.5) and shows mean and best fit paths in which rocks at the top of the Kaibab uplift resided at a temperature of ~100°C at the beginning of the Laramide orogeny (80 Ma), corresponding to a depth of burial of 3-4 km of overlying Mesozoic strata (using 20-25°C surface T and 20-25°C/km geothermal gradient). This

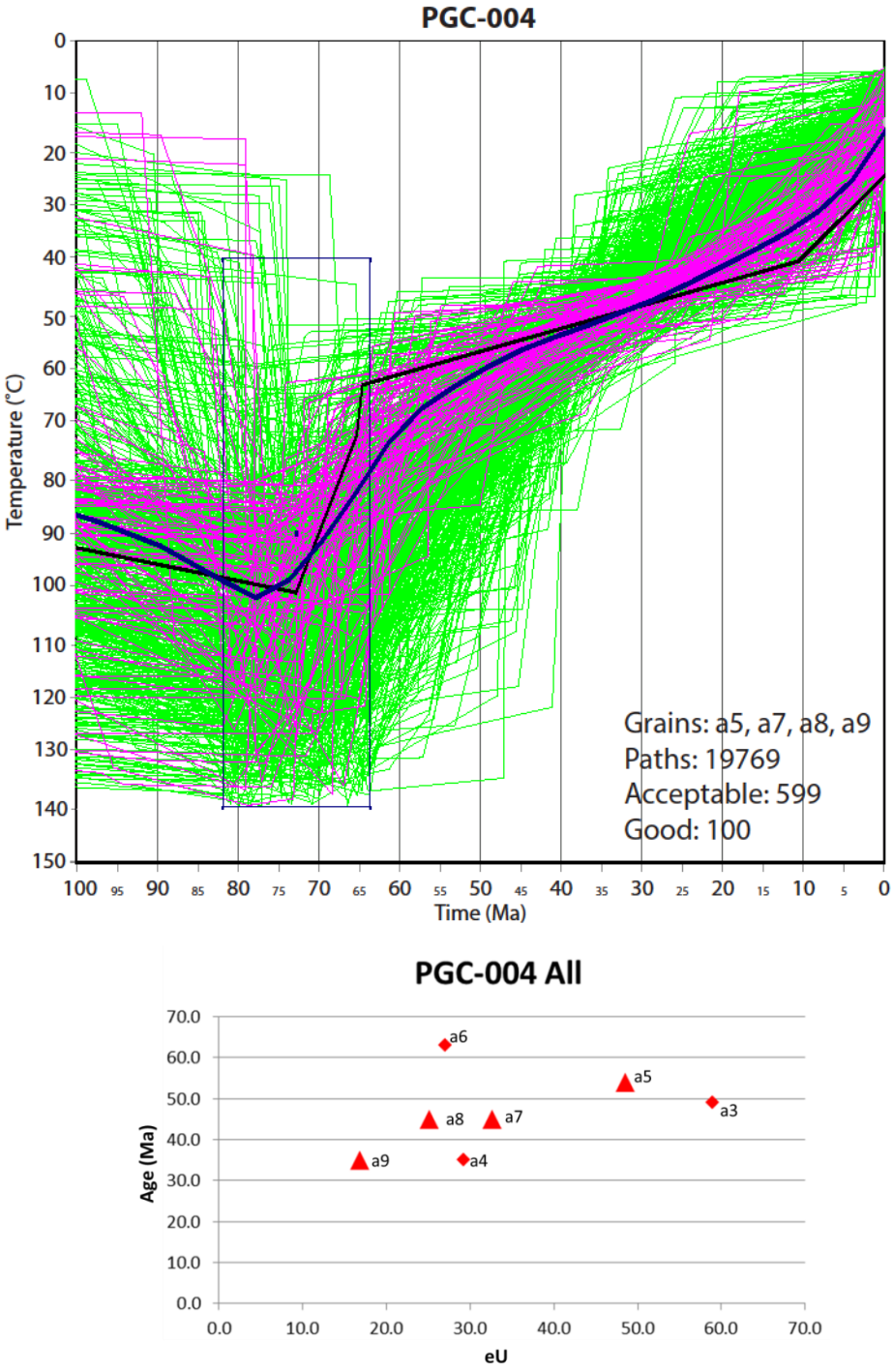

Figure 6. HeFTy plot for PGC-004 from 100 Ma to present and 0-150°C with inset of grain ages and eUs for entire sample. Grains used are shown in plot as triangles while grains which could not be modeled in the set are shown as diamonds.

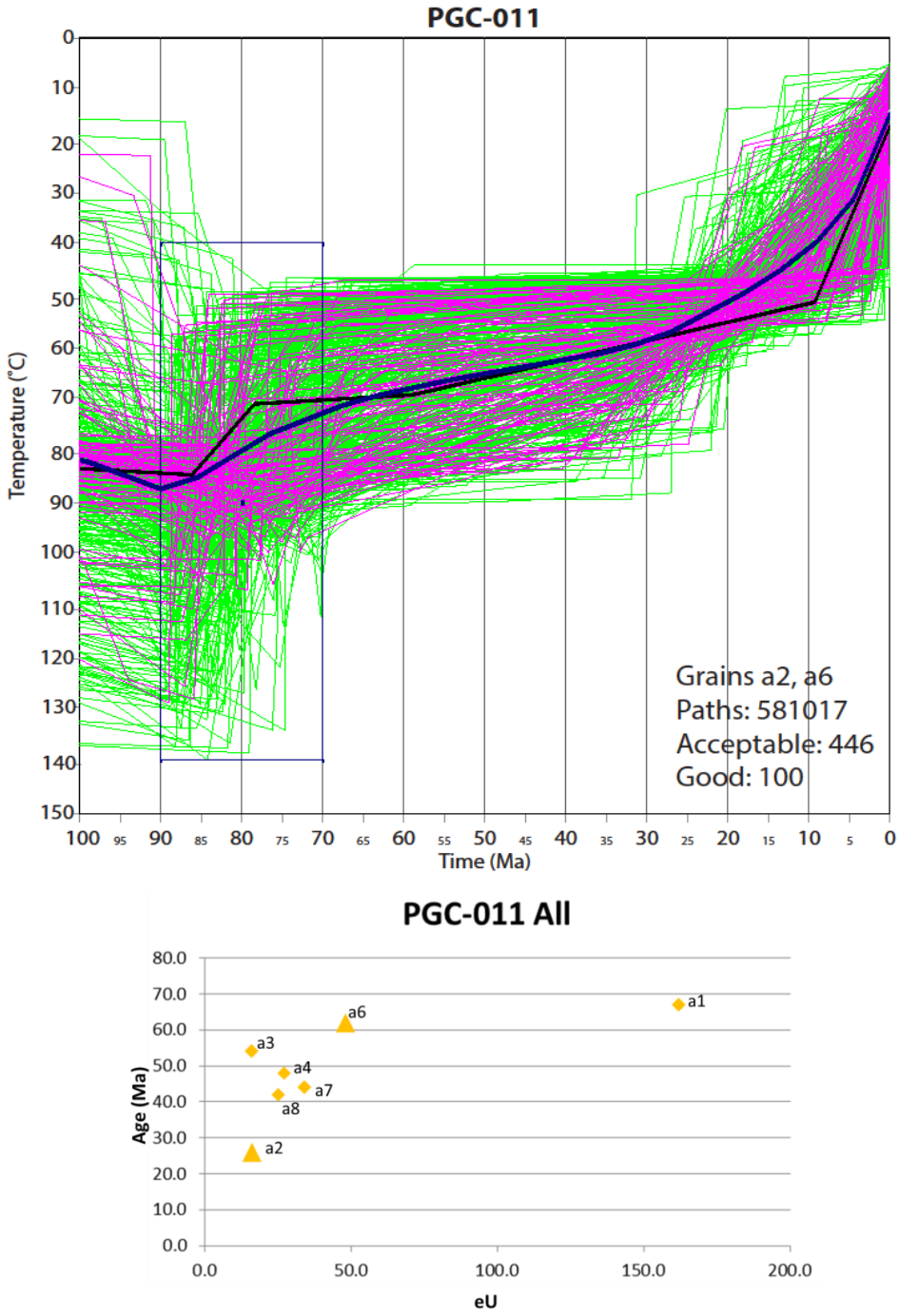

Figure 7. HeFTy plot for PGC-011 from 100 Ma to present and 0-150°C with inset of grain ages and eUs for entire sample. Grains used are shown in plot as triangles while grains which could not be modeled in the set are shown as diamonds.

sample shows two stages of cooling. The first episode of cooling begins at approximately 85-75 Ma. The grains are cooled to ~70°C by 60 Ma, then underwent a period of slow cooling (60 to 40°C) from 60 to <20 Ma. A second stage of more rapid cooling took place after about 20-10 Ma, but the exact time of onset of this later cooling is not well constrained by young grains (the youngest grain is 35 Ma); however, both weighted mean and best fit paths suggest 20 to 25 Ma cooling. The Laramide episode of cooling (~30°C of cooling), based on depth below the top of the Cretaceous, is interpreted to be due to erosional removal of 1.5 km of Cretaceous strata, followed by continued slow post-Laramide denudation of the region. The second stage of cooling, from 40°C to surface conditions, represents erosion of an additional 1 km of Jurassic and Triassic strata in the between 20 to 25 Ma.

PGC-011, from the Esplanade sandstone 100 m lower in the section than PGC-004, had seven grains analyzed (Flowers et al., 2008) and I was able to get only two to model together in HeFTy (Fig. 7). Nevertheless, along with comparison boxes for the other grains, it shows a very similar two-stage cooling since the Laramide. The first stage of cooling occurs between 85 and 55 Ma, when the sample was cooled ~60°C. This temperature was maintained until onset of rapid cooling in the last 20-25 million years. As with PGC-004, the first stage of cooling is interpreted to result from the denudation of the Cretaceous and Jurassic strata above the area and second stage cooling was from stripping of the remaining Jurassic and Triassic strata.

PGC-006 is also from the Esplanade Sandstone. Nine grains were analyzed (Flowers et al., 2008) but I was only able to get three to model together in HeFTy. This model also shows Late Cretaceous burial temperatures of 100°C, then a two stage cooling (Fig. 8) similar to PGC-004 and PGC-011. The sample shows a period of Laramide cooling from

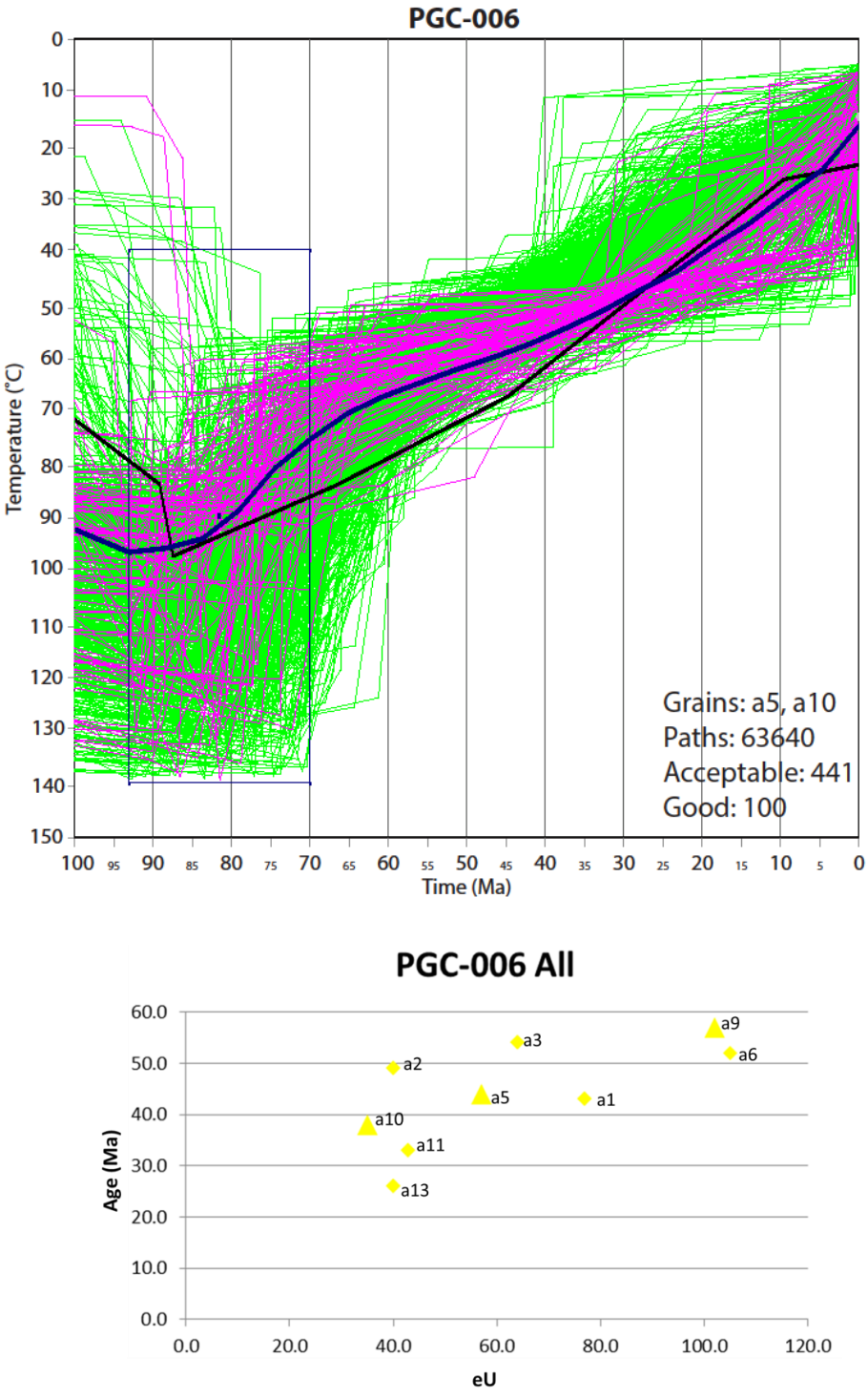

Figure 8. HeFTy plot for PGC-006 from 100 Ma to present and 0-150°C with inset of grain ages and eUs for entire sample. Grains used are shown in plot as triangles while grains which could not be modeled in the set are shown as diamonds.

85-70 Ma followed by slow cooling and residence in the AHe partial retention zone between 70 and 30 Ma, and a post-30 Ma cooling component. The timing of the late cooling episode is poorly constrained in this sample as the youngest AHe age is 26 Ma.

Sample PGC-002, also from the Esplanade Sandstone, has 7 grains analyzed (Flowers et al., 2008). It shows similar characteristics to the rest of the Kaibab uplift samples in the area (Fig. 9), and is maintained at similar temperatures between cooling events. Similar to sample PGC-006, the timing of onset of the late cooling episode is constrained to be after 19 Ma, the youngest AHe age.

Figure 10 shows a summary of all thermal history models for the four Kaibab uplift samples. All models of my samples are in good agreement, and they agree with the Flowers et al. 2007 model for PGC-004 in terms of pre-Laramide temperature and post-Laramide residence and slow cooling at ~ 60°C. The Flowers and Farley (2012) model disagrees with the rest in showing little Laramide cooling and post-Laramide residence at higher temperature (~ 80°C). Both of the Flowers models show Tertiary cooling beginning 25-15 Ma. The youngest AHe age from these samples is ~ 20 Ma (Fig. 5) and the models do not discriminate well between 25-15 versus post-10 Ma for the most recent cooling episode to effect these highest elevation samples. Differences of stratigraphic level between 004 (Coconino) and the Esplanade samples (002, 006, 011) show it cooling slightly later in the Laramide, but the overlap in the models is substantial and the resolution of the mean paths is unlikely to be this sensitive.

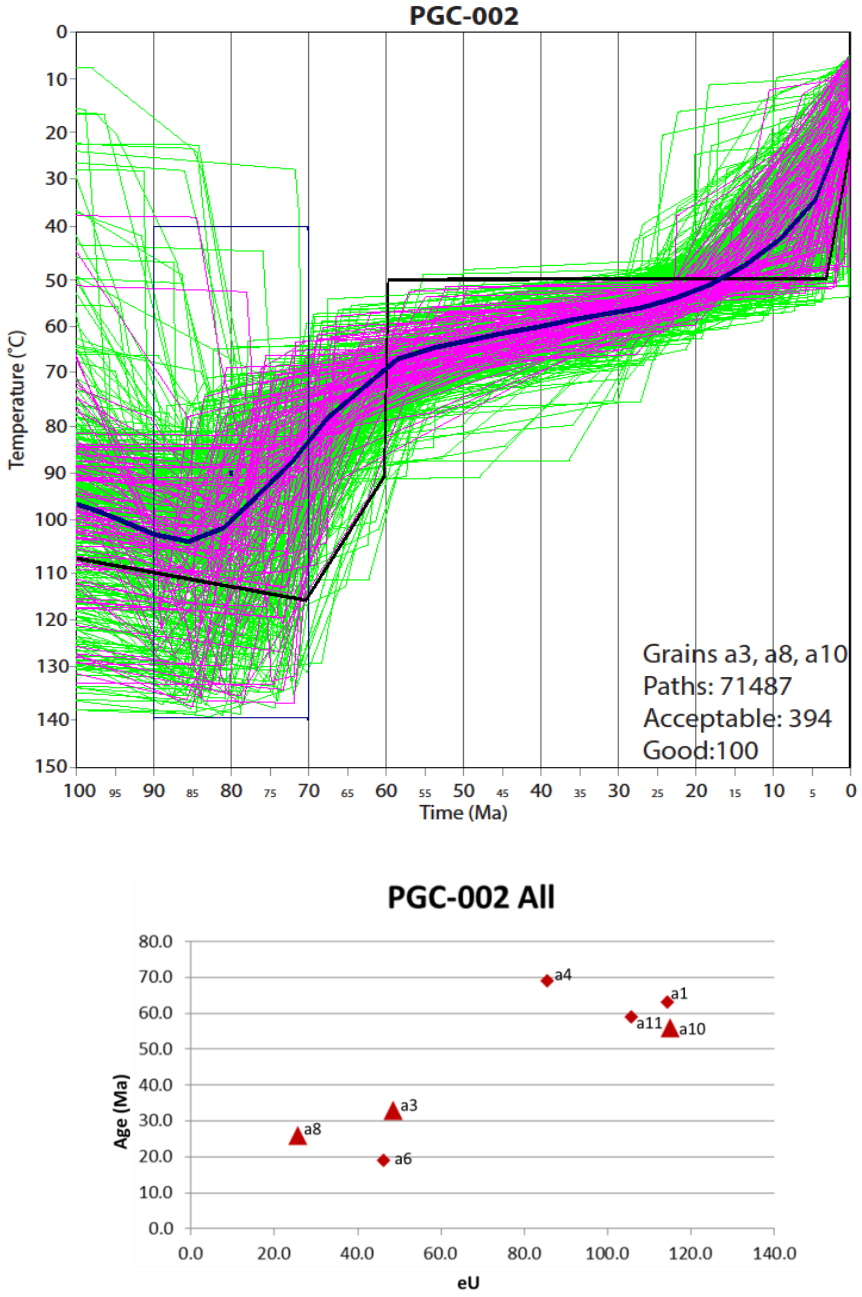

Figure 9. HeFTy plot for PGC-002 from 100 Ma to present and 0-150°C with inset of grain ages and eUs for entire sample. Grains used are shown in plot as triangles while grains which could not be modeled in the set are shown as diamonds.

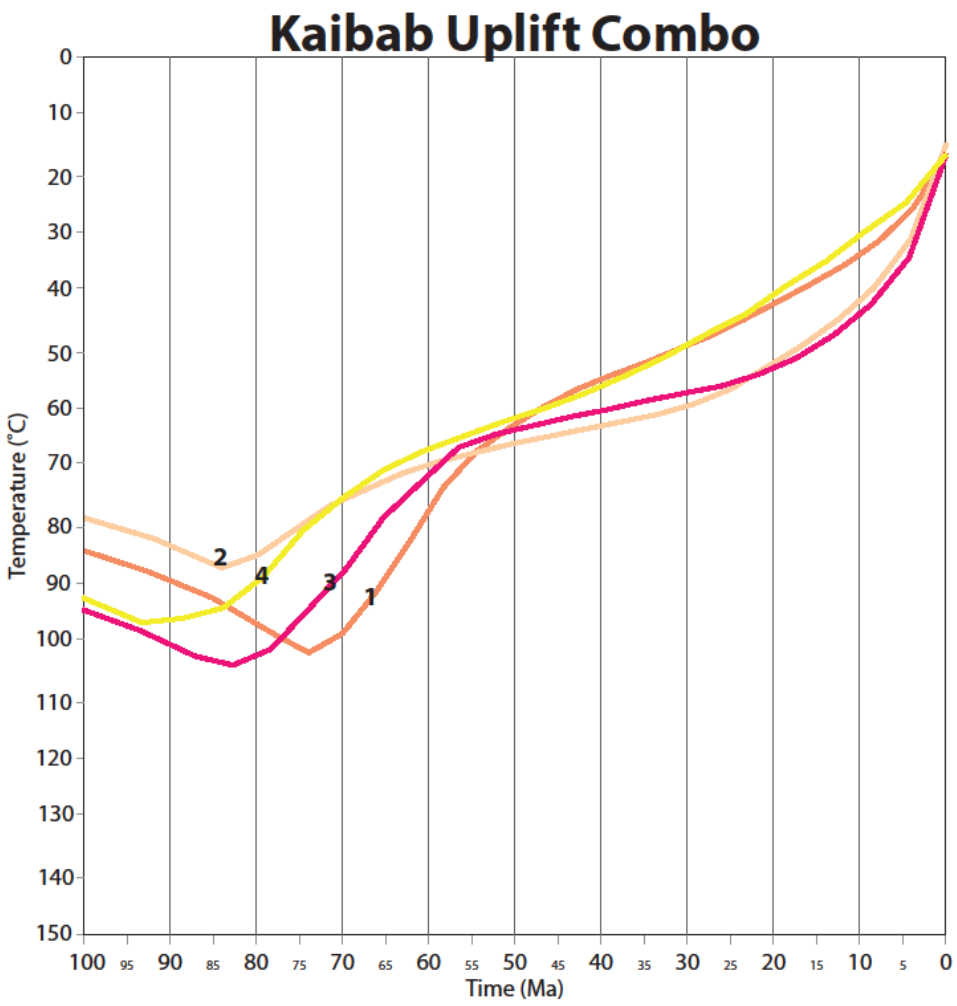

Figure 10. Combination of weighted mean paths from Flowers Kaibab Uplift samples: PGC-002, PGC-004, PGC-006 and PGC-011, numbers correspond to Table 1.

Kanab Creek samples

Two samples were taken by Flowers et al. (2008) from the Moenkopi Formation north and west of the Kaibab arch in the headwaters of Kanab Creek on the North Rim of Grand Canyon (Fig. 1). These samples are nearly a km lower in elevation than the Kaibab uplift samples yet at ~ 275 m higher stratigraphic position because they are on the west side of the west Kaibab fault zone. They are in very close proximity to each other, at the same elevation and, same stratigraphic position and hence must have had the same cooling histories relative to each other. PGC-015 had 19 grains analyzed; PGC-016 had 13 grains. The best model for PGC-015 (Fig. 11) had four grains that modeled together. It shows pre-Laramide temperatures of 90°C, cooling to 60°C in the Laramide (85-55 Ma), then long term residence at 55ºC between 55 and 10 Ma, the rapid cooling to near surface conditions in the last 6-10 Ma. Sample PGC-016 has 3 grains that modeled together to produce essentially the same cooling history. The mean cooling history for these samples indicates warmer temperatures compared to those from the top of the Kaibab uplift (Figs. 10 and 12). In this case, the younger cooling episode is well constrained by AHe ages as young as 5 Ma. Cretaceous rocks were removed from the crest of the Kaibab Uplift, but remained at Kanab until <10 Ma. The absence of post 19 Ma AHe ages in the Kaibab uplift samples may suggest that they cooled through AHe closure temperatures of 40-60°C at 20 Ma and that the uplift was denuded earlier than the surrounding synclinal down-dropped regions.

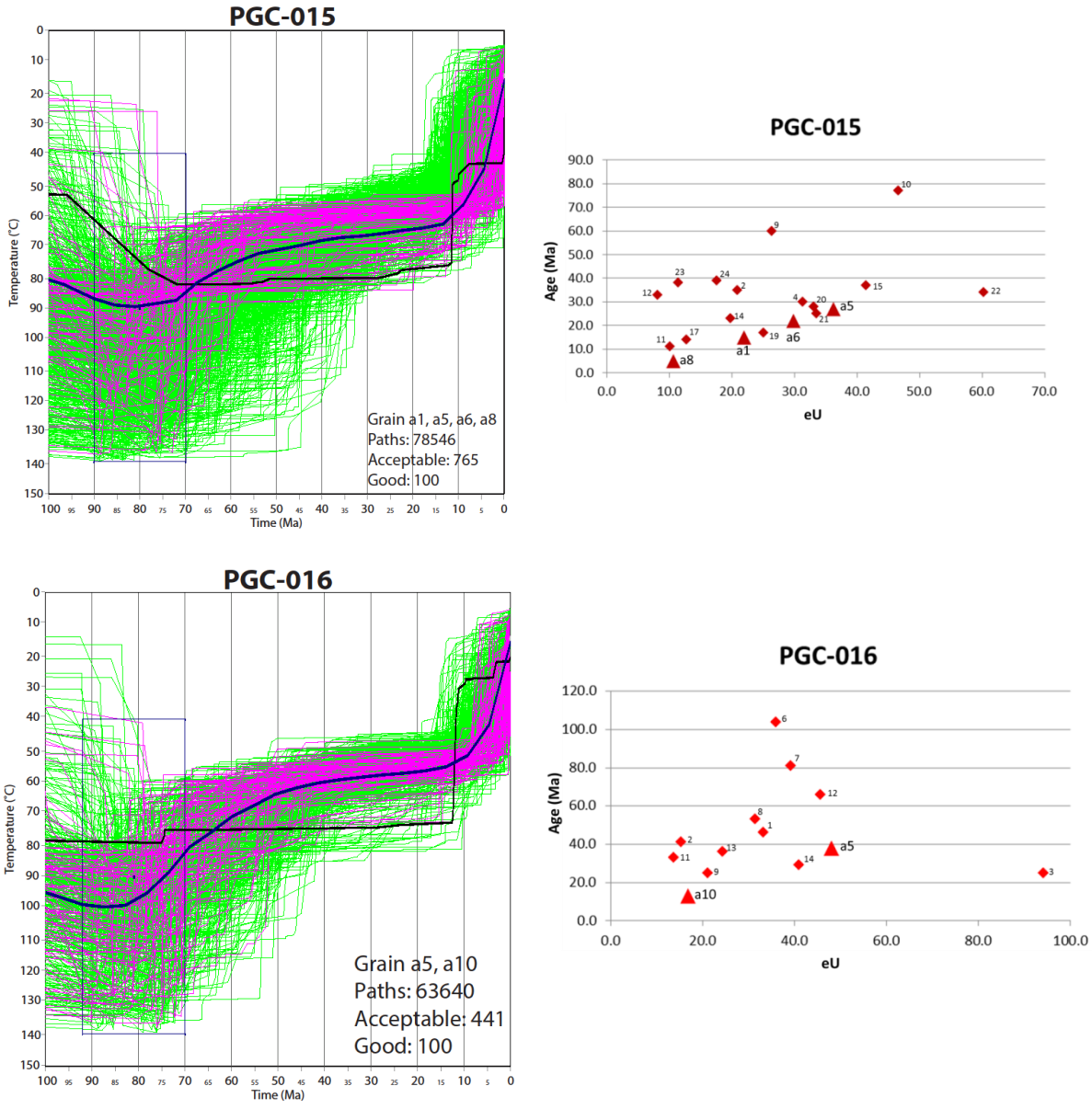

Figure 11. HeFTy plots for PGC-015 and PGC-016 from 100 Ma to present and 0-150°C with inset of grain ages and eUs for entire sample. Grains used are shown in plot as triangles while grains which could not be modeled in the set are shown as diamonds.

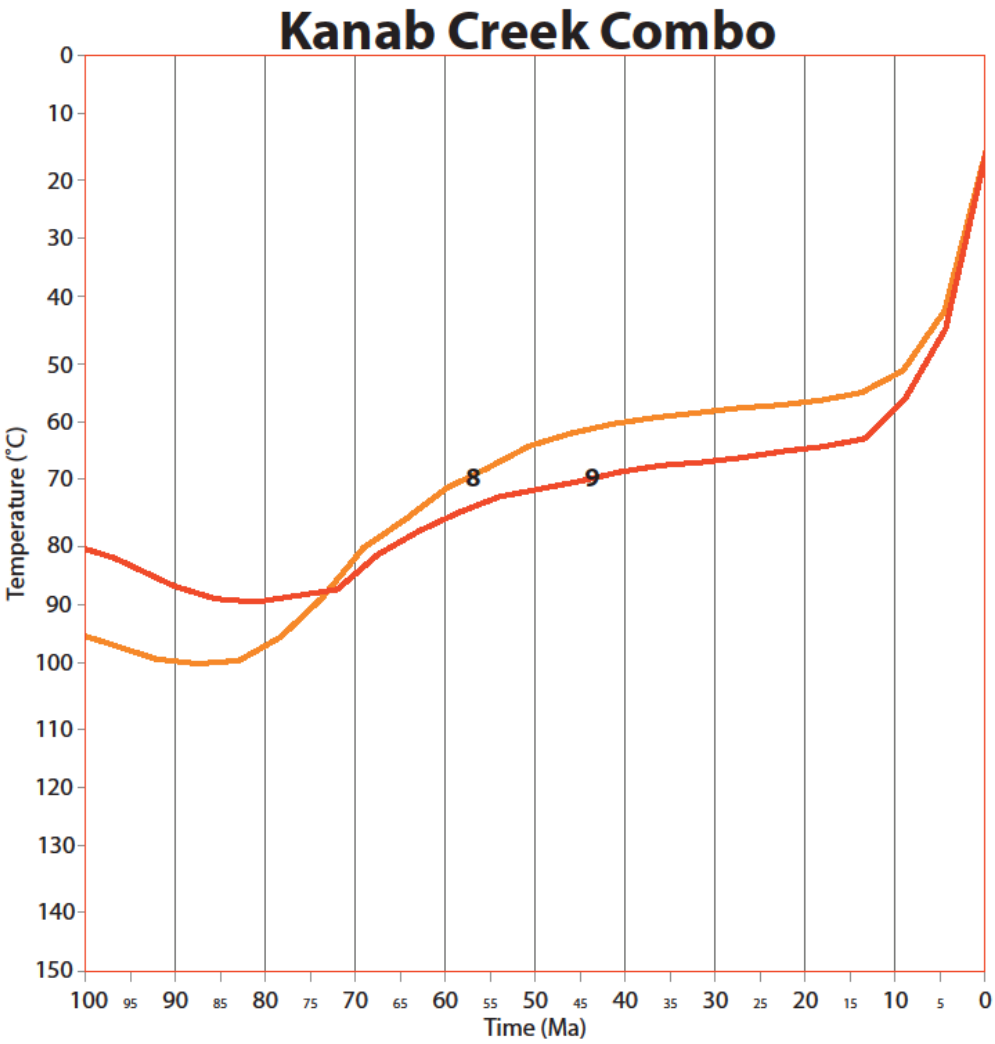

Figure 12. Combination of weighted mean paths from Flowers Kanab Creek samples: PGC-015 and PGC-016, numbers correspond to Table 1.

Vermilion Cliffs samples

K11-VC-2052 is a single grain analysis from the top of the Vermilion cliffs. Its age is 73.4 Ma and its eU is 21.9, one of the lower values for samples from this study. Thus, a traditional interpretation of this age is that the rock cooled through ~50ºC at 70 Ma, during the Laramide orogeny. This is compatible with other high elevation samples from the Kaibab uplift (Fig. 5). A single grain Hefty model is shown in Figure 13, which shows that best paths for this grain cooled through varied potential cooling temperatures of 40-70°C at the grain age (with uncertainty) of 70-76 Ma. Post-Laramide cooling is unconstrained, but I conclude that the top of the Vermilion Cliffs in this location was covered by a minimum additional 0.6 to 1.8 km of Cretaceous strata at 70 Ma (using 25°C and 25°C/km) or 1- 2.5 km using (20°C and 20°C/km).

K11-VC-1790 is from the same traverse (Sand Crack on Vermilion cliffs), but is 262 m lower in the Mesozoic section (still in the Navajo Sandstone). This difference in elevation in the same transect would equate to a 5 ºC difference in temperature within what would be expected to be a similar cooling history. This sample has three analyzed grains, two of which modeled together (Fig. 14). The model shows Laramide temperatures of ~ 100°C at 70 Ma (significantly hotter than K11-VC-2052) and essentially no Laramide cooling, but significant cooling 40-25 Ma. All of the grains are 30- 35 Ma (and low eU) such that timing of rapid cooling is after 30 Ma, but not well constrained by these samples. Single grain comparison boxes are compatible with the two grain model.

All of the Vermilion cliffs and Marble Canyon river corridor samples are considered together by compiling mean paths in Fig. 21B. This follows an assumption that all these samples should show similar shaped cooling paths because of their close proximity, but with perhaps a 10-12°C offset reflecting their 500m differences in elevation. The combined data

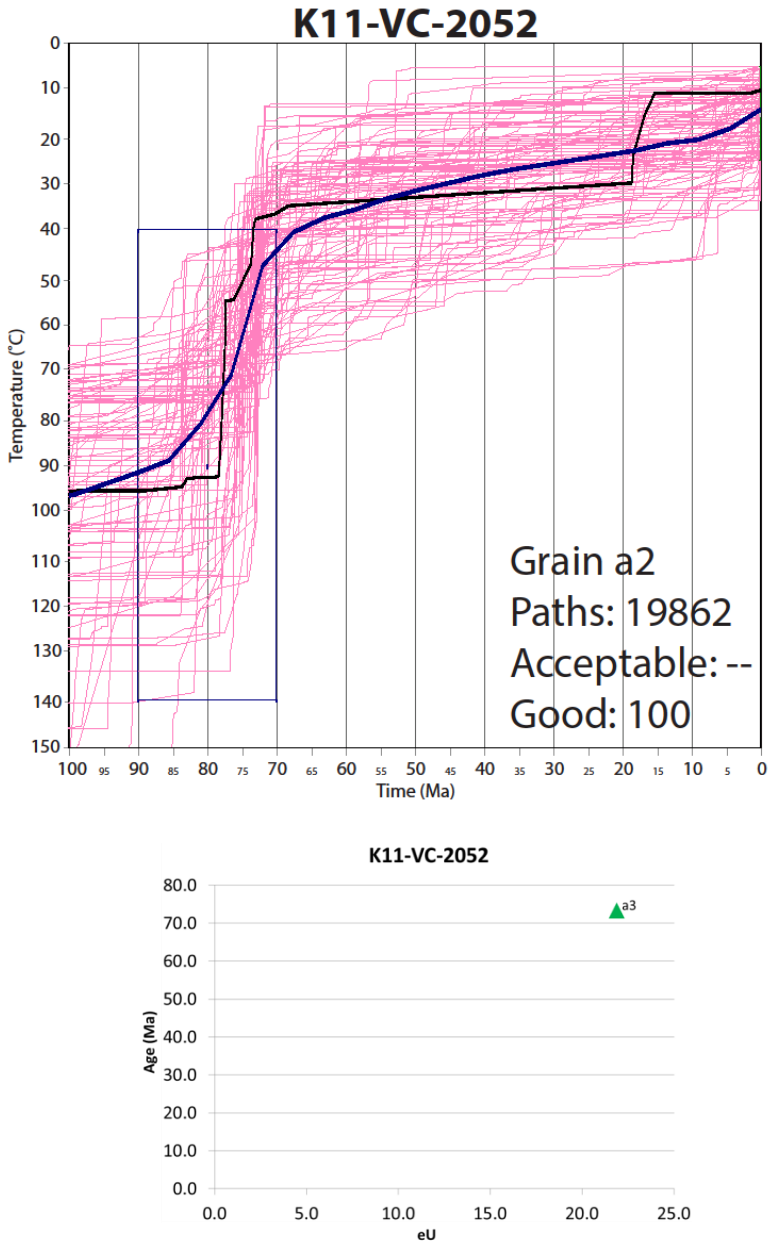

Figure 13. HeFTy plot for K11-VC-2052 from 100 Ma to present and 0-150°C with inset of grain ages and eUs for entire sample. Grains used are shown in plot as triangles while grains which could not be modeled in the set are shown as diamonds.

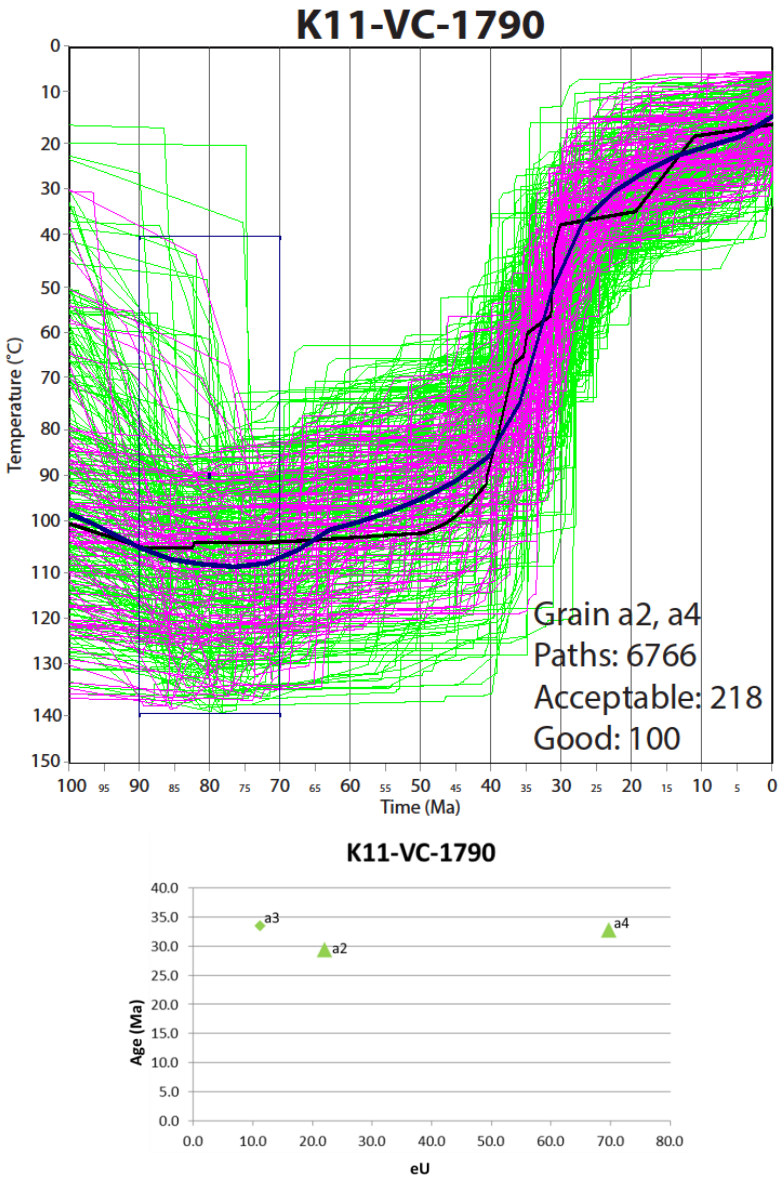

Figure 14. HeFTy plot for K11-VC-1790 from 100 Ma to present and 0-150°C with inset of grain ages and eUs for entire sample. Grains used are shown in plot as triangles while grains which could not be modeled in the set are shown as diamonds.

suggest a cooling path shape that involved a two-stage cooling history, with both a Laramide and mid-Tertiary component and a 50-30 Ma residence within the partial retention zone.

Kaibab rim of Marble Canyon

Rim and river samples were obtained from a previously un-sampled stretch that corresponds to the main segment of Marble Canyon, from river mile 12 to 50. Samples from South Canyon fill an important gap in the Lee et al. (2013) river level samples, and are from the same location as the Polyak et al. (2008) speleothem data. K12-32-South4 is from South Canyon (River Mile 32) at an elevation of 1593 m, about 700 m above the river and in the Kaibab Formation near the rim of Marble Canyon. This is a key location to test the apparent upstream progression of cooling ages shown by Lee et al. (2013) in which samples from near the confluence between the Colorado River and Little Colorado River (RM 66.3) cooled rapidly from 25-20 Ma, and a sample at RM 11.6 cooled rapidly during nearly the same time interval 20-15 Ma. This suggests that intervening samples near river level (half way between these samples) should have also cooled in the 25-15 Ma interval. This area has carbonates at river level, but the 700 m difference in elevation between rim and river here can be used to hypothesize that a rim sample might have a cooling history similar to a river level sample, except offset about 14°C. This sample had three apatite grains that were analyzed and models were successful with two grains that had very different eU values (Fig. 15). The resulting models differ depending on which grain is paired with a2. The a2, a5 pairing shows a progressive cooling history whereas modeling with as and a4 shows steady temperatures between 70 and 20 Ma. Post Laramide cooling from about 100°C is compatible with other samples from this reach. Importantly, the 20 Ma (youngest) grain suggests cooling of the sample through 40-70°C at 20 Ma such that

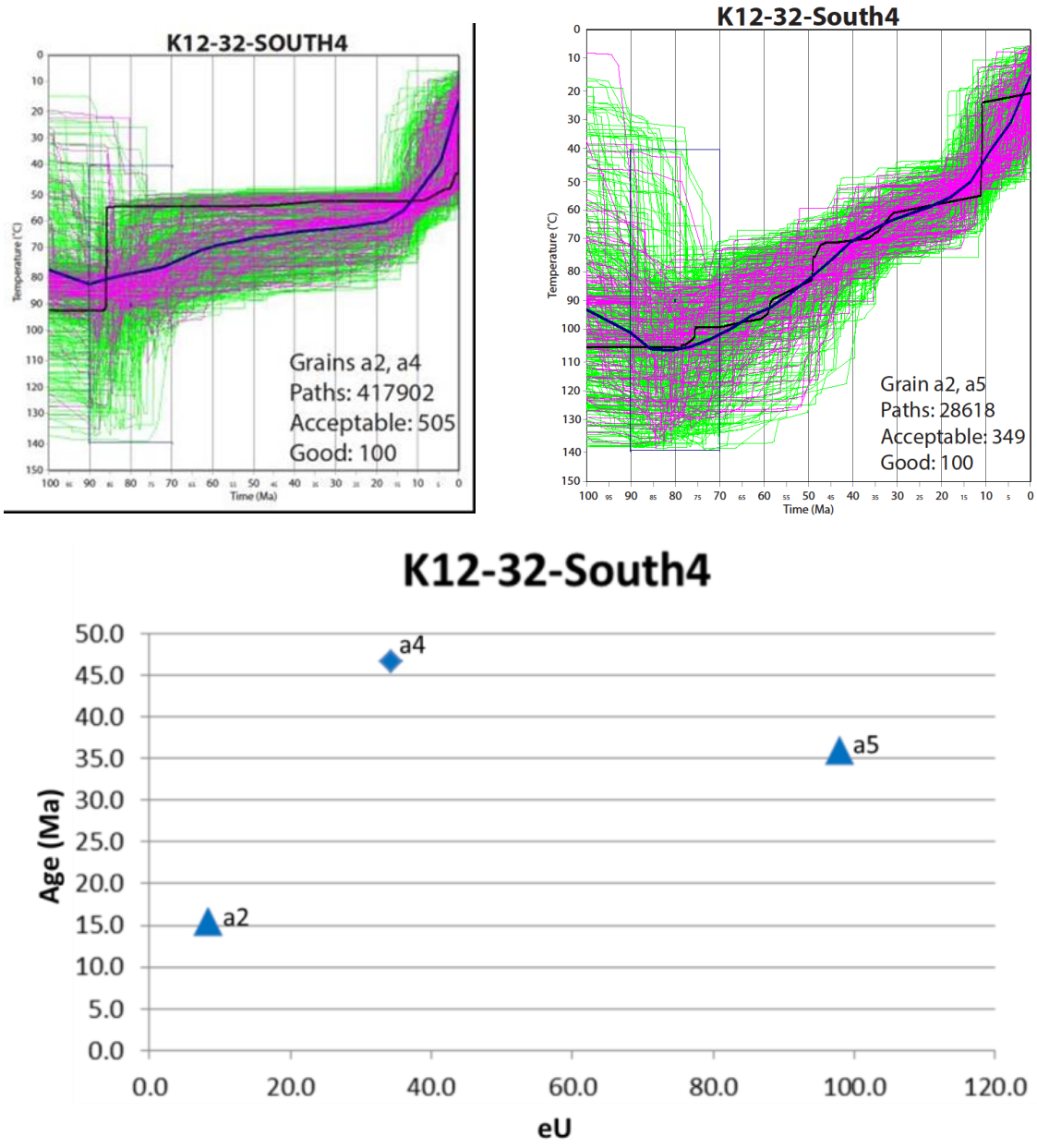

Figure 15. HeFTy plots for K12-32-South4 from 100 Ma to present and 0-150°C with inset of grain ages and eUs for entire sample. Grains used are shown in plot as triangles while grains which could not be modeled in the set are shown as diamonds.

I infer that the Kaibab Limestone surface in this region was covered by a minimum additional 0.6 to 1.8 km of Jurassic strata (using 25°C and 25°C/km) or as much as 1- 2.5 km (using 20°C and 20°C/km).

K12-32-South7 comes from the Supai Formation along the trail to South Canyon (river mile 32). It is at an elevation of 1214 m, 369 m below K12-32-South4 and 347 m above the river. This sample should show a similar pattern to that of K12-32-South4 (Fig. 16), but offset 5-10°C (within the uncertainty of my models). This sample has two 20-25 Ma grains and single grain models suggest likely cooling through 40-70°C at this time. These models show rapid cooling within the time frame of 25-15 Ma, in agreement with other samples. Hence I infer that the Vermilion cliffs Jurassic section had not retreated north of this location until after 20 Ma, in agreement with the > 60°C estimated AHe temperatures for samples near the base of the Vermilion cliffs discussed above.

Samples from Soap Creek (RM 11)

Progressing upstream, K12-SC1 (Fig. 17) is a sample from the Kaibab surface at the rim of Soap Creek (river mile 11) in Marble Canyon. This sample is 314 m higher in elevation than river level sample 01GC93 and would be expected to show a similar cooling path but offset to ~ 10°C higher temperature. The age-eU relationships are inverse of expected relationships in the RDAAM model as grains with older age have lower eU, which is possible in times of rapid cooling when all grains cool within a narrow timeframe. However, two grains have an age of about 20 Ma, and were modeled together suggesting a likely temperature range of 40-60°C at this time. The sample ran with those two grains,

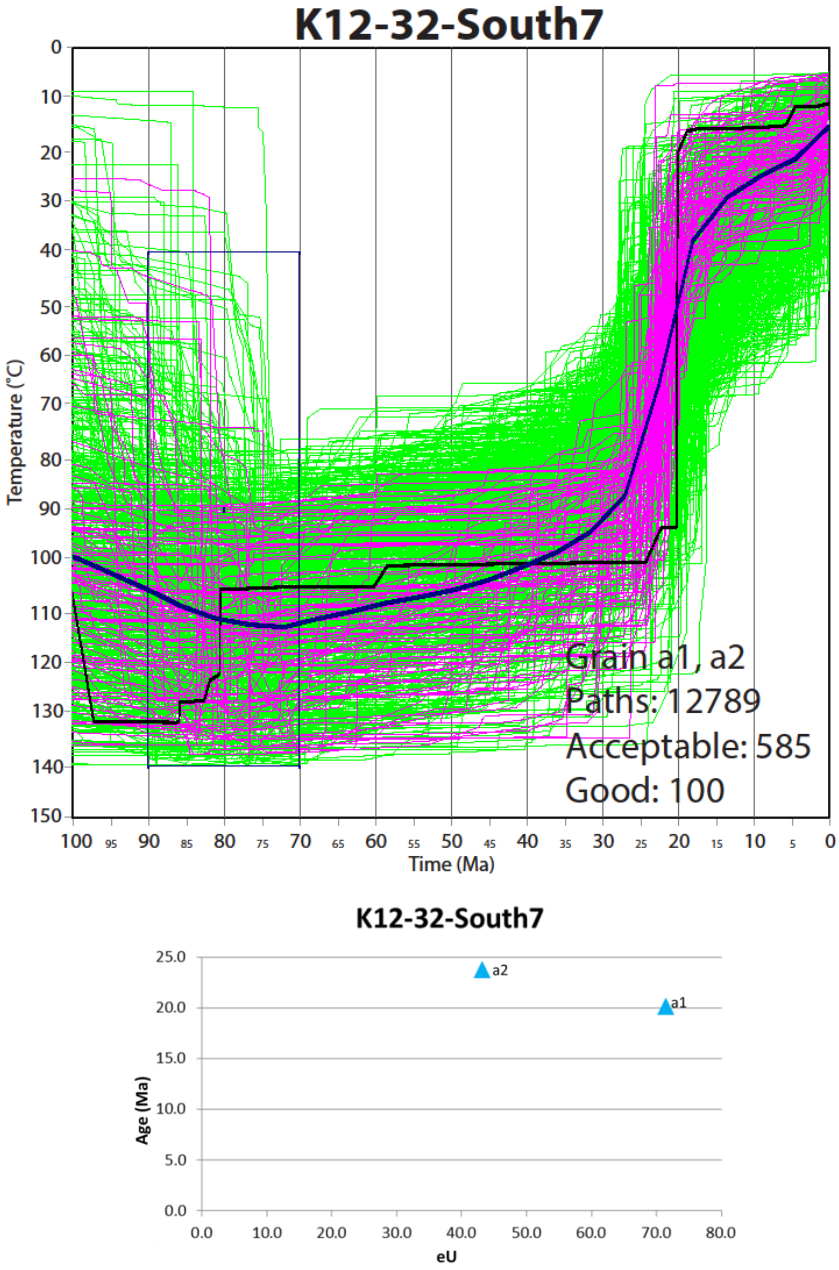

Figure 16. HeFTy plot for K12-32-South7 from 100 Ma to present and 0-150°C with inset of grain ages and eUs for entire sample. Grains used are shown in plot as triangles while grains which could not be modeled in the set are shown as diamonds.

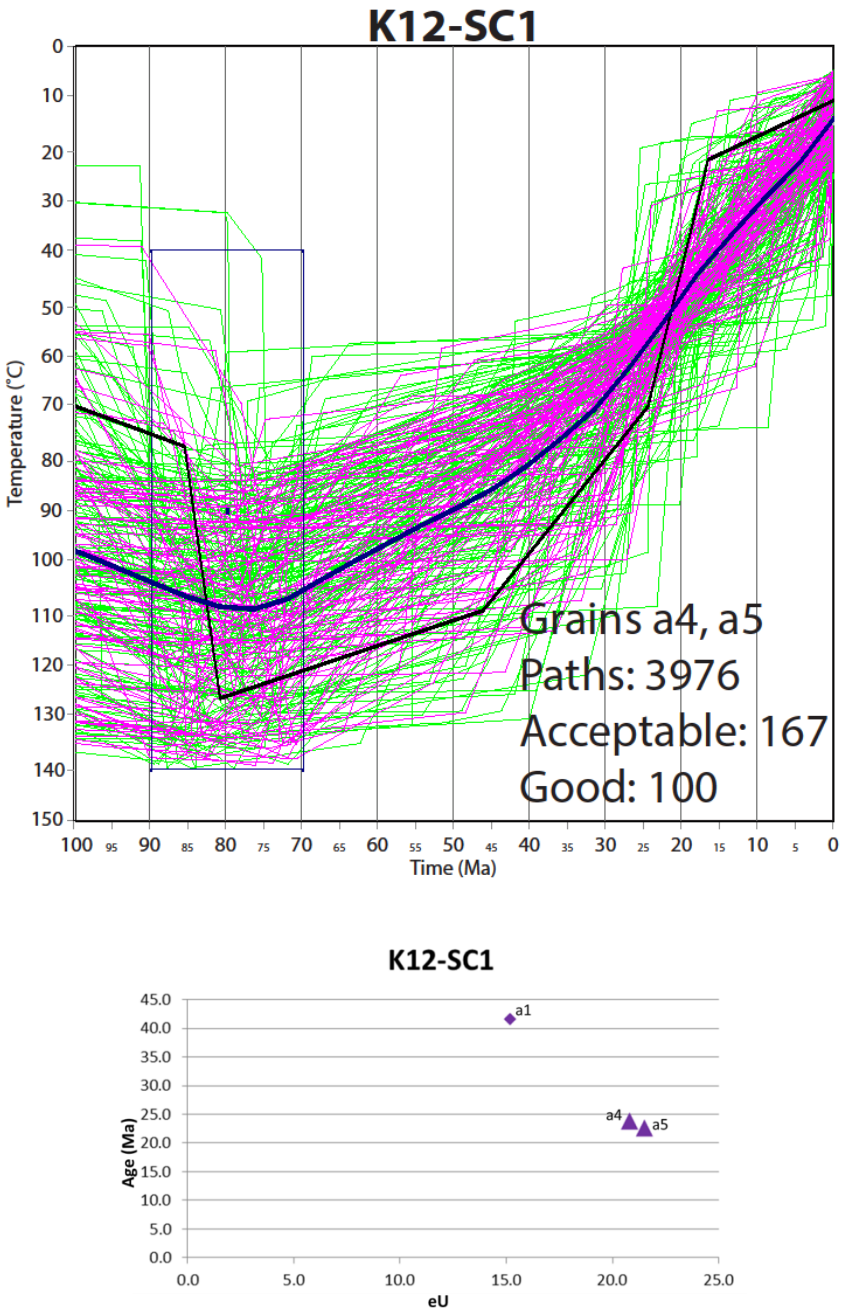

Figure 17. HeFTy plot for K12-SC1 from 100 Ma to present and 0-150°C with inset of grain ages and eUs for entire sample. Grains used are shown in plot as triangles while grains which could not be modeled in the set are shown as diamonds.

a4 and a5. Though the sample's weighted mean line shows slow and steady cooling over the course of the last 50 Ma, the best fit path shows a possible increase in rate of cooling at 25-15 Ma that agrees with the South Canyon history, which indicates that the Vermilion cliffs Jurassic section extended across the present Kaibab surface until after 20-15 Ma.

The river level sample from this location was presented by Lee et al. (2013) using both AFT and AHe data (Fig. 18, 19, 20). These workers used a slightly different set of geologic constraint boxes for the modeling that started models within an assumed 80-120 ºC box for early Laramide time (80 – 75 Ma). However, my new models use the same constraint boxes as my other samples and give similar results (see Appendix A). My model for 01GC93 was based on three grains plus the AFT data from the river level at Soap Creek. In agreement with the Lee et al. model, mine shows rapid cooling from ~100°C to 40°C between 25 and 15 Ma (Fig. 20).

Lees Ferry region

Two additional samples were analyzed by Lee et al. (2013) from river level from uppermost Marble Canyon, near Lees Ferry: 01GC90; river mile zero and 01GC92; river mile 3. I remodeled these samples using the same geologic constraint boxes as my other models for consistency in comparing cooling histories from place to place. The models are similar to the Lee et al. models (2013), with a few differences. Models for 01GC90 (three AHe) and 01GC92 (four AHe) show both 25-15 and post-6 Ma cooling episodes. Samples near Lees Ferry did not record the Laramide cooling and hence were above 110ºC until 40 Ma, but showed a two stage cooling history involving 30-20 Ma and post 6 Ma episodes.

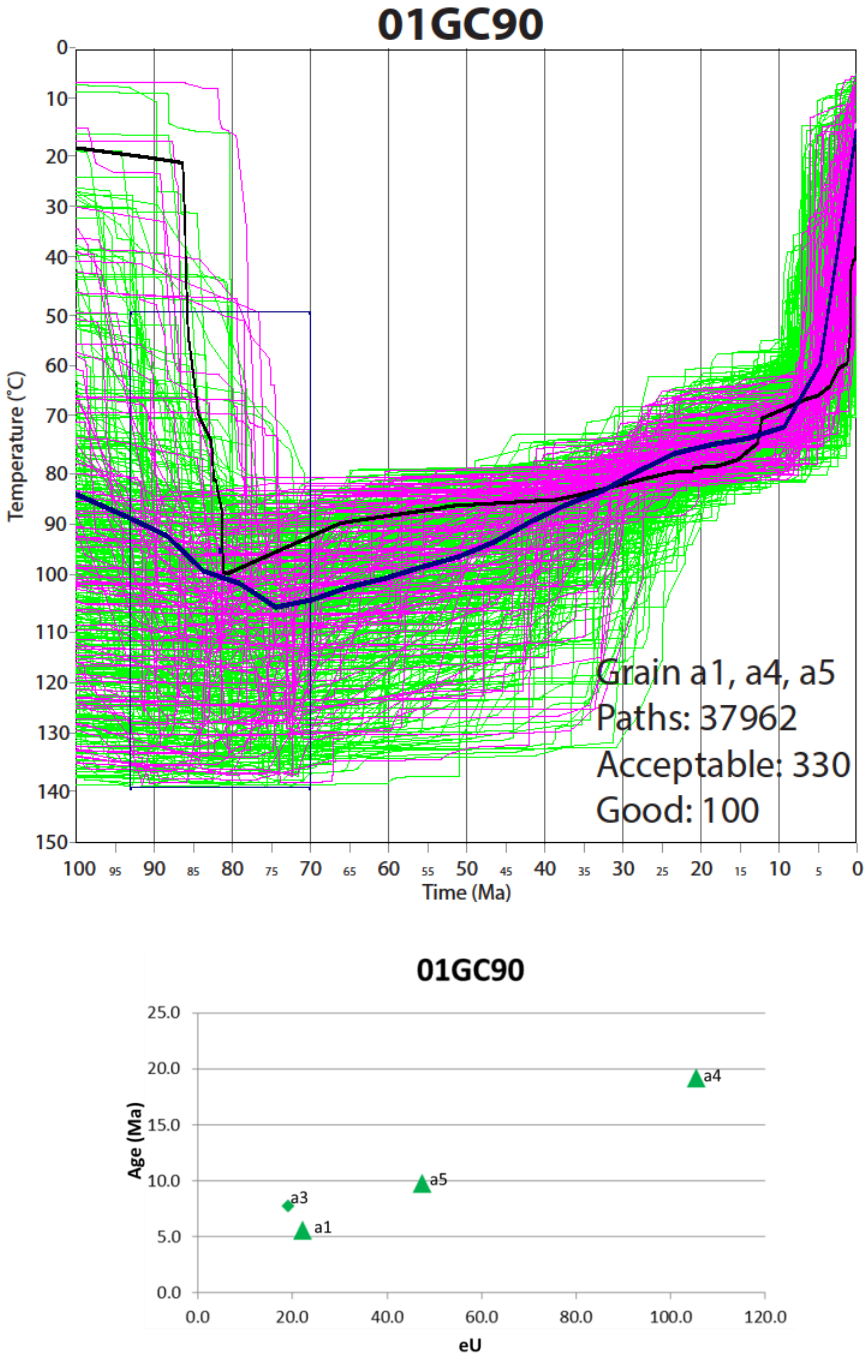

Figure 18. HeFTy plot for 01GC90 from 100 Ma to present and 0-150°C with inset of grain ages and eUs for entire sample. Grains used are shown in plot as triangles while grains which could not be modeled in the set are shown as diamonds.

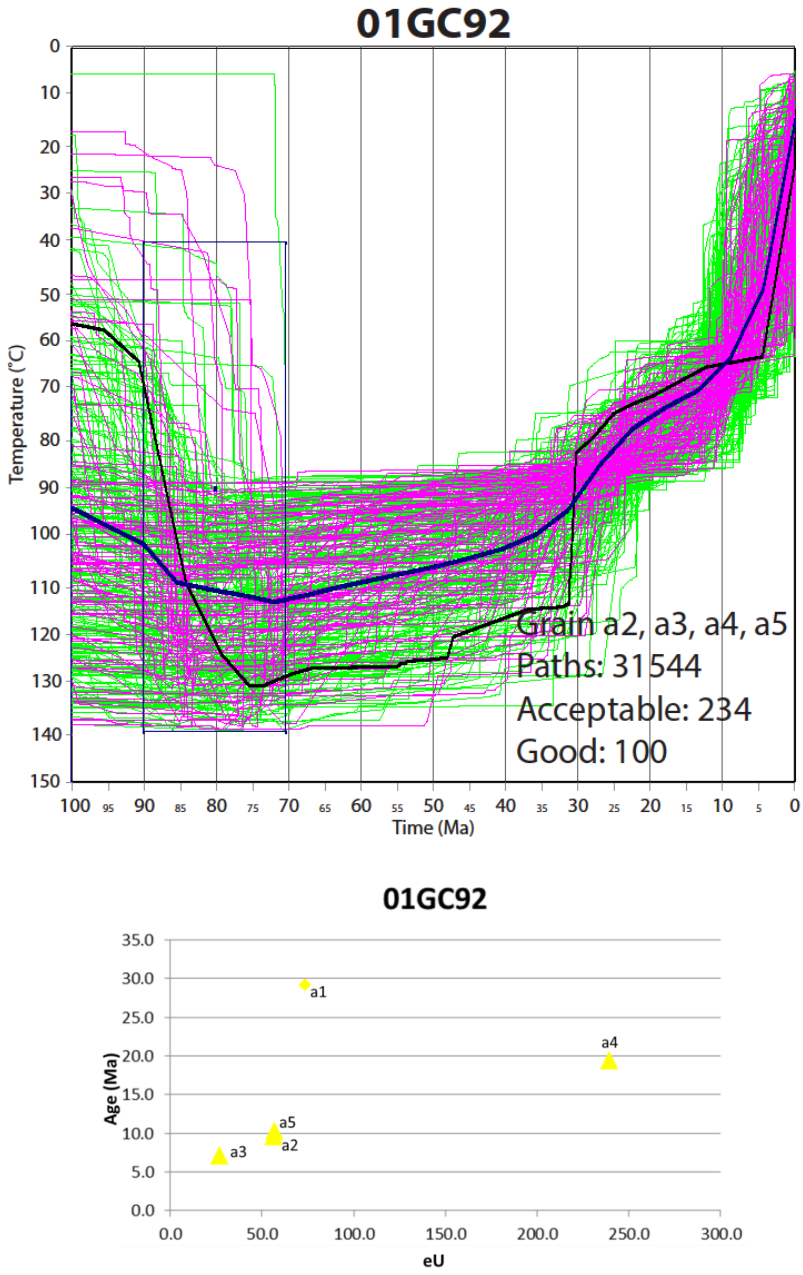

Figure 19. HeFTy plot for 01GC92 from 100 Ma to present and 0-150°C with inset of grain ages and eUs for entire sample. Grains used are shown in plot as triangles while grains which could not be modeled in the set are shown as diamonds.

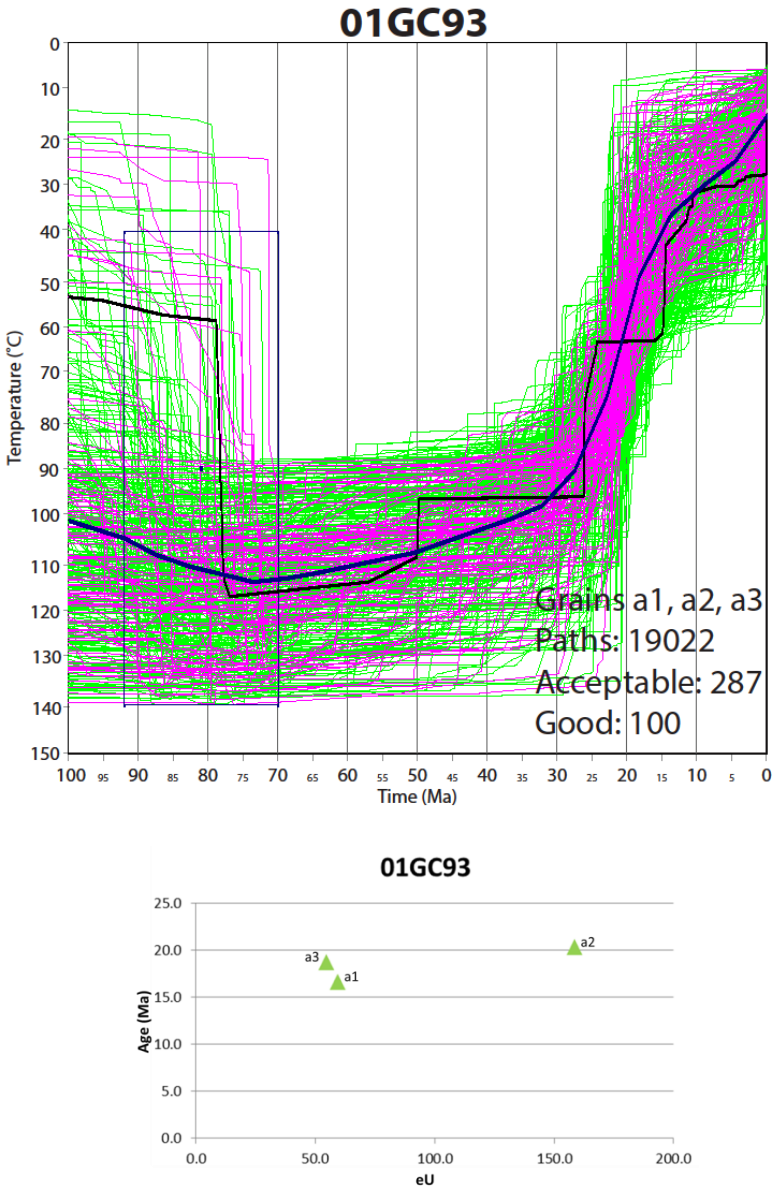

Figure 20. HeFTy plot for 01GC93 from 100 Ma to present and 0-150°C with inset of grain ages and eUs for entire sample. Grains used are shown in plot as triangles while grains which could not be modeled in the set are shown as diamonds.

INTERPRETATION OF COOLING PATHS

The cooling paths presented above fall into several geographic groupings that provide information about regional stripping of the Kaibab surface and carving of Marble Canyon. These are summarized and interpreted from SW to NE to test alternative models (Fig. 2) for timing of incision of paleorivers and cliff retreat of the SW Colorado Plateau.

The combined South Rim samples from Lee et al. (2013) show a similar cooling history for all the samples on the stripped Kaibab surface south of Grand Canyon. These are summarized here in the context of testing the Flowers et al (2008) model for SW to NE stripping of the Kaibab surface. A summary of the Lee et al. (2013) models from Karlstrom et al. (2014) shows important differences between these samples (Figure 21B). The region near the Little Colorado confluence has a two-stage cooling history, with post Laramide cooling at 55-50 Ma, then cooling related to carving of the East Kaibab paleocanyon across the Kaibab Uplift at 25-20 Ma. Figures 1, 10, and 12 show the locations and mean cooling paths for 6 samples. A progressive SW to NE sweep of denudation, for instance due to cliff retreat, would predict that the order of cooling would be 21,20,(19,16,17),18,(7,15), using sample numbers from Table 1. Instead, models strongly overlap and do not suggest this order. Rather, within the resolution of the models, all samples appear to have cooled from 100 to 70°C from 90-70 Ma during the Laramide orogeny, which I interpret to be due to erosional denudation of ~1.5 km of Cretaceous rock from this area. The region then cooled very slowly from 70-60°C between 70 and 25 Ma, interpreted to reflect slow erosion of another 500 m of Cretaceous rock. The region then cooled more rapidly from 60-30°C between 25 and 15 Ma,

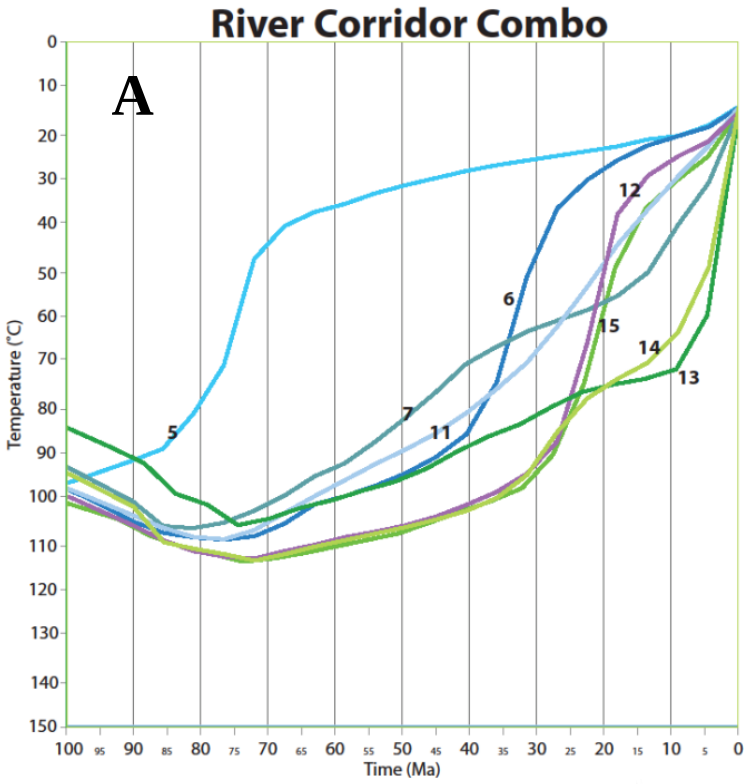

B

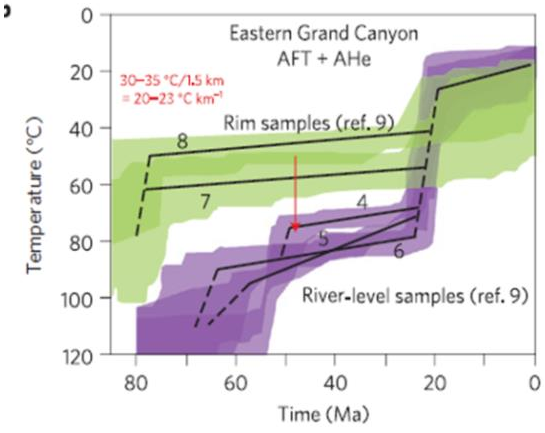

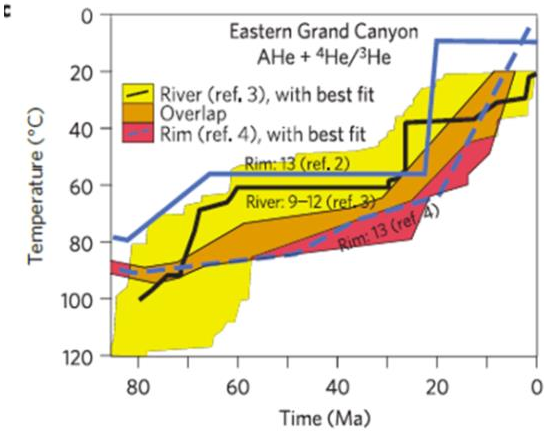

Figure 21A. Combination of Vermillion Cliffs, Kaibab Surface and River Level weighted mean paths. 21B. Summary of models from Lee et al. (2013) as shown in Karlstrom et al. (2014)

which I interpret to be a response to base level lowering following the 25-15 Ma carving of East Kaibab paleocanyon and erosional removal of the 1.5 km thick Jurassic section from the south Kaibab surface. The Kaibab surface cooled to <30°C in the last 10 Ma which I interpret to reflect erosion of the 500 m thick Triassic section, remnants of which are still present at Red Butte near the south Rim of Grand Canyon and beneath the San Francisco volcanic field.

The combined North Rim- Kaibab uplift samples (Fig 8) also show a two-stage cooling history involving Laramide cooling of ~40 ºC between 90 and 70 Ma, long term slow cooling of ~10 ºC between 70 and 20 Ma, then rapid cooling from 50 ºC to surface temperatures (assumed to be 20 ºC) in the last 20 Ma. Samples PGC-011, PGC-006, PGC-004 and PGC-002 from the Kaibab uplift and GCNK1 from North Rim are assumed to have had similar cooling histories because they are in close proximity, near the same elevation, within 200 m of each other stratigraphically, and not separated by significant faults. This reasoning allows me to use the best constrained of the models as well as the weight of the multiple models to refine the best constrained cooling path. PGC-011 had 4 grains that modeled together with tightly grouped best fit models. Its range of ages of grains 26 to 67 Ma and eU (16-162) provide good constraints for both the Laramide and post-20-25 Ma cooling episodes and the 70 Ma intervening period of slow cooling within the AHe partial retention zone. My interpretation of these cooling paths is that the Kaibab uplift samples were at >100°C prior to the Laramide orogeny which corresponds to a burial depth of 4 km of Mesozoic rock (using 20°C surface temperature and 20°C/km geothermal gradient). It cooled from 100 to ~70°C between 90 and 70 Ma due to erosional denudation of 1 km of Cretaceous rock from this region. The region was then relatively stable with slow cooling from 70 to 60°C reflecting about 500 m of erosion of Cretaceous rocks 70 to 20 Ma. After 20 Ma, the

uplift cooled from 60°C to near surface temperature (20°C) due to erosional denudation of 2 km of Jurassic and Triassic rocks. Present data do not closely constrain whether the Kaibab uplift samples started cooling ~ 25 Ma or <10 Ma as indicated by the Muddy Creek constraint. Additional data are needed to refine models for whether the uplift was stripped in two stages (25-15 and < 10 Ma) or a single episode (<10 Ma). My preferred model, based on data from all around the uplift, is that the Cretaceous section was stripped 25-15 Ma due to first-stage retreat set up by carving of the East Kaibab paleocanyon, then additional stripping of the remainder of the Mesozoic section took place after Colorado River integration in the last 6 Ma, based on the Muddy Creek constraint.

The combined Kanab Creek cooling paths are from samples at much lower elevation on the NW side of the Kaibab uplift (Fig 12). They are younger than the Kaibab Uplift samples. The Kaibab uplift was formed in the Laramide and was draped on the flanks by a substantial portion of Mesozoic section. The region was denuded in two pulses; the first at 25-15 Ma near the east Kaibab paleocanyon and the other at post-10 Ma at the flank. The Kanab samples are especially important in documenting the later episode, as grain ages get as young as 5 Ma. These show that the Jurassic section (Vermilion cliffs) covered this region until after 5 Ma and the retreat of the Grand Staircase in this region has taken place predominantly in the last 5 Ma.

The combined Marble Canyon river level samples indicate that most of the Marble Canyon region was at >100°C until after 40 Ma, which I interpret to reflect burial by about 4 km of sedimentary rock including the entire Cretaceous section on the down-warped side of the Kaibab monocline. The combined data suggest that Marble Canyon had little Laramide cooling and instead had the complete Cretaceous section on top of it until after 25 Ma. Two

major cooling episodes are recorded in Marble canyon rocks. Rim and some river samples (below river mile 3.5) cooled by ~40 ºC between 25 and 15 Ma. I interpret this to reflect erosional removal of 2 km of Cretaceous rocks from this area. The river level samples also show this 25-15 Ma episode as a dominant time of cooling as far upstream as Soap Creek (RM 11). However, the notch in the Vermilion cliffs apparently formed in the last 5-6 Ma based on the very young grains near Lees Ferry.

EPISODIC COOLING OF THE MARBLE CANYON REGION

From the presented and analyzed data, I infer 3 major episodes of cooling in the Marble Canyon region. Rapid cooling is seen first in the Laramide, between 80 and 50 Ma. This first event is seen in almost all samples (except Lees Ferry samples) regardless of elevation. The second event was mid-Tertiary (25-15 Ma) and is seen in some river level rocks, as well as near the base of the Vermilion cliffs. The Kaibab Uplift samples probably underwent cooling at both 25-15 Ma (crest) and < 10 Ma (flank), but available thermochronology does not constrain times of onset of rapid cooling very well. Kanab drainage samples, and the most northerly river level samples (Lees Ferry), show cooling in the past 6 million years.

Laramide: ~ 40°C of Laramide cooling is evident in many of the samples; the samples with an obvious Laramide-aged event occur in the Flowers et al. (2007 & 2008) samples. The Kaibab Uplift and Kanab Creek samples show the most cooling during this time, possibly due to the removal of the upper 1-2 km of strata, i.e. the Cretaceous section, shown in the stratigraphic column in figure 3A. The South Rim Grand Canyon and south Kaibab plateau samples also record this time of cooling.

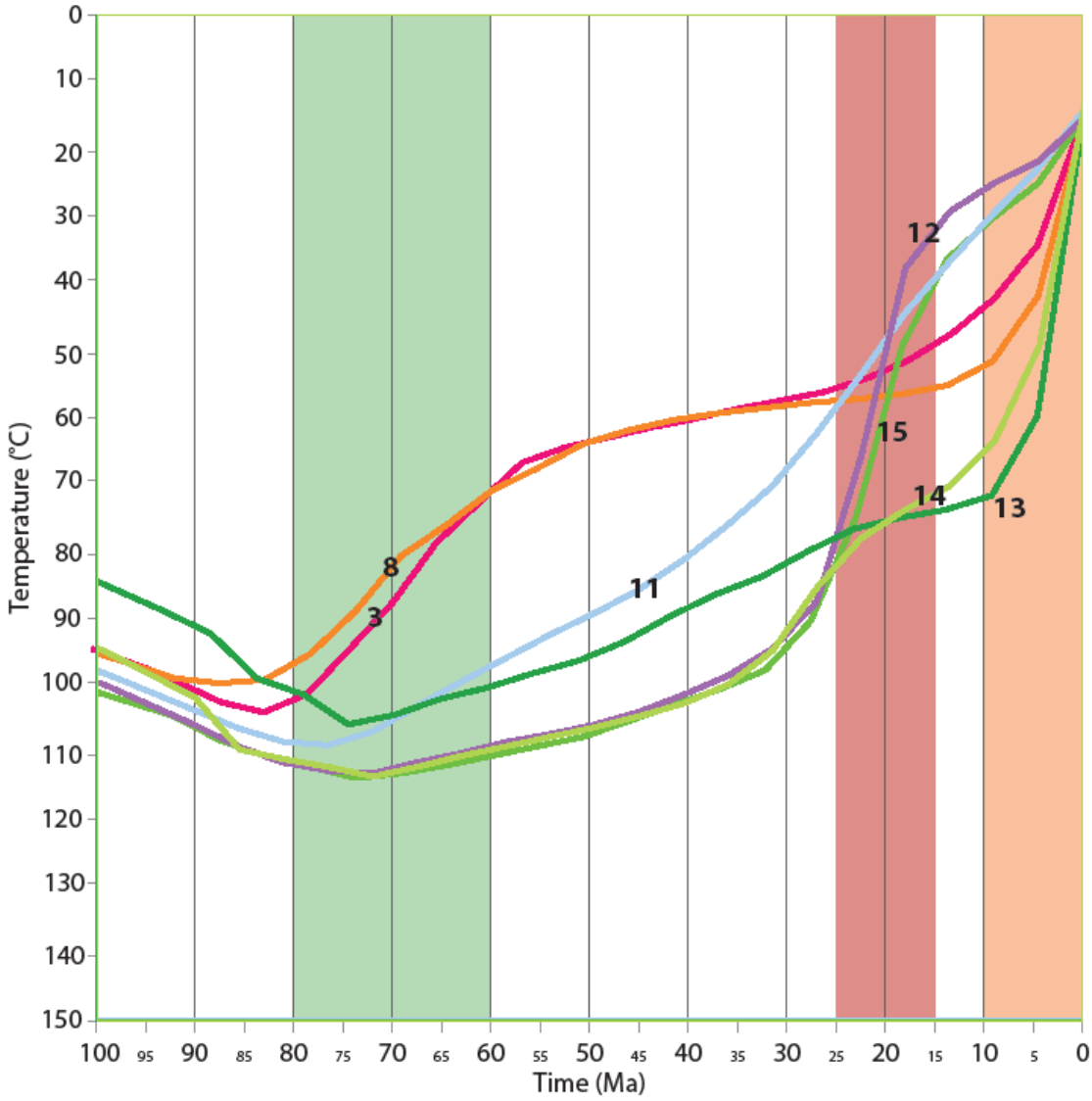

Figure 22. Combination of representative weighted mean lines from samples in all areas of the study. Numbered lines correlate to sample numbers in Table 1. Colored boxes represent reasonable times of rapid denudation in the region. Green represents post-Laramide cooling, red represents 15-25 Ma cooling and orange represents post-10 Ma cooling.

Mid- Tertiary (25-15Ma): The rapid cooling in the mid-Tertiary is one best observed in the river corridor, along the rim of the canyon, and in the Vermilion Cliff samples. This cooling episode interrupted a time of tectonic stability and slow cooling across the region and involved about 20-40°C of cooling in river level samples. This is interpreted to record retreat of the rest of the Mesozoic section from the south Kaibab plateau, top of the Kaibab Uplift and region of the Kaibab rim of Marble Canyon as far upstream as Soap Creek (RM 11), and the Vermilion cliffs. This is the time period when the cooling paths of river level rocks across the Kaibab uplift (from River Mile 60 to 115) merged (became the same temperature as) with rim samples(Lee et al., 2013; Karlstrom et al., 2014b). This pattern is depicted in Fig 22 and suggests that East Kaibab paleocanyon was carved at this time across the Kaibab uplift. The overall 25-15 Ma pattern of denudation, and its importance regionally is best explained by retreat of the rims of the 25-15 Ma East Kaibab paleocanyon rather than a unidirectional northward cliff retreat.

Post 10 Ma: The most recent, episode of cooling seen in HeFTy models from this study are those paths which cooled from 75 to 25°C within the past 10 million years. This cooling episode is seen across the Marble Canyon region, in the river corridor samples and those at Lees Ferry in the far northeastern stretch of the Grand Canyon. This rapid denudation shows that a significant vertical section of rock was removed rapidly from the present day surface in the last 10 million years. This is the same timing as onset of rapid cooling in the Monument Uplift along the San Juan River and the Book Cliffs along the Colorado River (Hoffman, 2009; Karlstrom et al., 2012) and is interpreted as due to incision across a drainage divide in the Lees Ferry area, and formation of the notch in the Vermilion cliffs near Lees Ferry due to integration of the Colorado River through older paleocanyons.

This event itself has been postulated to be due to mantle-driven uplift of the Rocky Mountains and western Colorado Plateau (Karlstrom et al., 2012).

Interplay between vertical (canyon carving) and horizontal (cliff retreat) erosion

Interpretations made from the cooling paths lead to new insights about mechanisms of erosional denudation. Continuous regional vertical denudation across the region as a mechanism of cooling/denudation can be ruled out, as this type of denudation would have produced steady cooling throughout the course of the plots and from one area to another. Instead, as summarized above, I see episodes of rapid cooling separated by times of very slow cooling with abrupt changes in cooling rate in the Laramide, at 25-15 Ma, and in the past 10 Ma.

Horizontal erosion via cliff retreat, if the dominant mechanism, would predict that large vertical sections of rock could be removed by erosion of weak layers and undermining of resistant cliffs to leave behind resistant surfaces like the Kaibab surface. In this model, cooling patterns in different areas should track the rates and direction of progressive removal of cliffs and episodicity of cooling would be controlled by cliff retreat. This is likely an important mechanism to promote episodic cooling, but data so far do not strongly show progressive stripping of the Kaibab surface in any particular direction. This also would require an additional mechanism such as base level or climate variations.

Current data seem most consistent with a combination and interplay between vertical incision of paleocanyons that trigger cliff retreat of rims. Vertical incision focused into local areas, rather than regional vertical incision, could be explained by river incision due to base level fall events and the formation of paleocanyons. When incision rates were high, rapid cooling would take place as the river system carried sediment away from the region,

vertically denuding the landscape. Rims of paleocanyons then should provide starting points for subsequent rapid cliff retreat, with geometries dictated by initial paleocanyon geometry. Given that the Colorado Plateau is characterized by a system of rivers and spectacular canyons today, this seems like a uniformitarian explanation for the Laramide and 25-15 Ma observed cooling episodes.

SYNTHESIS AND CONCLUSIONS

The three cooling periods discussed above (80-70 Ma, 25-15 Ma, and post 10 Ma) are all interpreted here as times of regional base level fall, probably driven by tectonic events. Each time period is known to have had important paleocanyons and paleorivers although their paths remain incompletely known. Hence, the conclusion in this synthesis is that geologically significant river/canyon carving events led to cliff retreat and that differential cooling data reflect these linked processes.

Laramide uplift and denudation patterns were dominanted by uplift of the Nevadaplano (DeCelles, 2004) to the west and Mogollon/Kingman highlands to the southwest (Beard and Faulds, 2011). The path of Laramide rivers is poorly known in detail, but rivers flowered north (Karlstrom et al., 2014) and northeast (Cather et al., 2012) toward the Green River basin (Dickinson et al., 2012) and/or San Juan Basin (Potochnik, 2001). 65-50 Ma paleocanyons reached 1 km deep (Young, 2001; Potochnik, 2001) and northward retreat of the north rim of Hindu-Old Man paleocanyon has been interpreted to have ultimately formed the modern Kaibab escarpment on the north rim of western Grand Canyon (Young and Hartman, 2014). Cooling data suggest that Laramide uplift and erosion resulted in stripping of a significant fraction of the Cretaceous section from the south Kaibab surface, north Kaibab uplift, and Kaibab Rim/ Vermilion Cliffs areas of Marble Canyon region. The

Kaibab uplift was not completely denuded to the Kaibab Limestone during the Laramide (Kelley and Karlstrom, 2012), and Cretaceous strata certainly remained on both the east and west flanks.

Thermochronologic data provide the best evidence for carving of an East Kaibab paleocanyon as shown by Lee et al. (2013) and Karlstrom et al. (2014) and in Figure 8. This paleocanyon is postulated to have been km-deep and to have carved an east-west paleocanyon across the Kaibab uplift, with its floor in Paleozoic rocks and rim in Jurassic rocks (on the south) and Cretaceous rocks on the North. The onset of cliff retreat from this paleocanyon in the 25-15 Ma interval, combined with the incision of the paleocanyon and formation of tributaries, is envisioned to have been responsible for cooling of South Kaibab surface and cooling of the Marble Canyon Kaibab rim.

The final episode of cooling, in the last 10 million years, is interpreted here to be due to the integration of Colorado River through older paleocanyon segments to form its present path in Grand Canyon, and resulting additional cliff retreat components. New models for the Kaibab uplift samples show that they cooled due to erosional unroofing of some of the Mesozoic section starting at 20 Ma. Similarly, Kanab drainage was also cooled due to erosion of much of the Cretaceous section in the last 10 Ma. A major conclusion of this paper is that the Grand Staircase as is seen today represents cliff retreat following Colorado River integration since ~5-6 Ma, when the integration of the Colorado River through the entire canyon is constrained by the age of the Muddy Creek Formation.

It is possible that the retreat of cliffs, which we now see in southeastern Utah as the Grand Staircase, caused the quick cooling in both 25-15 and post-6 Ma episodes. If the cliffs were stripped back from this region, in a geometry similar to that of today, a given location

might record removal of a 1-2 km of Cretaceous strata, then removal of Jurassic and Triassic sections. Regions like the Zion plateau have the entire section preserved, but wide benches on weak rocks at the top (Tropic shale) and base (Chinle Formation) of the Jurassic section suggests the possibility of a two stage process in some regions.

Marble Canyon itself is very young, carved since 10 Ma due to Colorado River integration as shown by the > 80°C temperatures of rocks of the Lees Ferry region until 5 Ma reflecting burial by 2-3 km of rock above the Kaibab Limestone hence strata preserved well into the Cretaceous section. However, thermochronologic data in some samples (notably 01GC92) here also record information about an earlier 25-15 Ma cooling episode. The present day geometry of the Vermilion and Echo Cliffs likely records aspects of both episodes. I infer ~ 40°C cooling between 25-15 Ma due to rapid retreat of Cretaceous section to near the position of the modern Vermilion cliffs, then retreat of the Cretaceous section, and additional retreat of the Vermilion cliffs, to their present positon in the last 5-6 Ma. The notch in the Vermilion cliffs was likely non-existent at 10 Ma, creating a smooth line from Echo to the Vermilion Cliffs. The thermochronologic data are consistent with very rapid initiation of carving of the Lee's Ferry region of Marble Canyon (as shown by samples 01GC90 and 92), but data are not yet sufficient to address downward (spill over and groundwater sapping) versus headward erosion integration mechanisms for the 5-6 Ma Colorado River.

Appendix A: Sensitivity tests and comparisons to previous modeled results

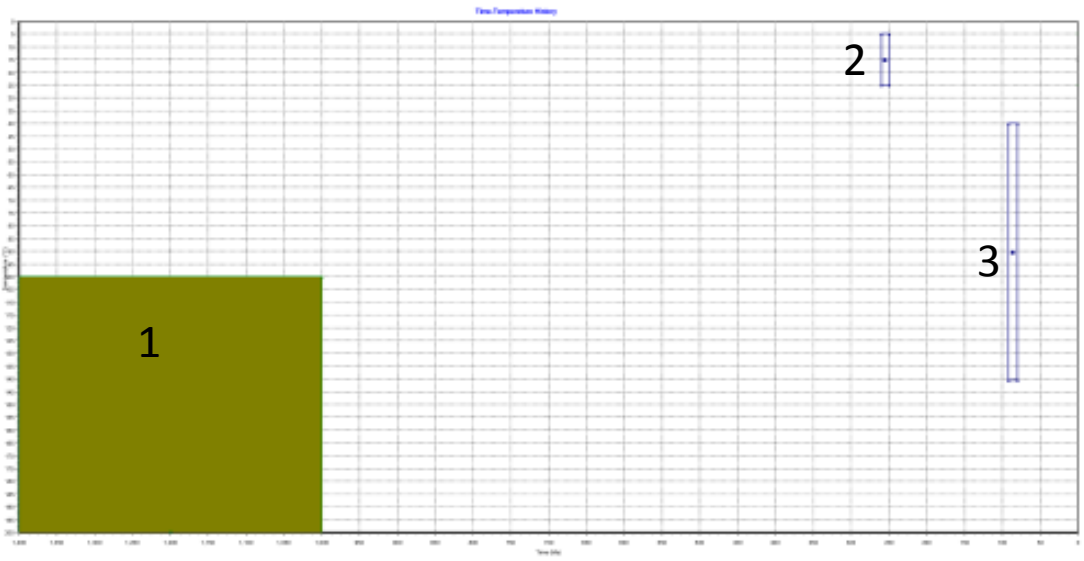

Constraint boxes used for modeling:

1) Cooling of apatites through 100-300 C; 1.4-1.0 Ga
2) Deposition of detrital apatites
3) Heating to 40-140 C , 90-80 Ma due to sed. Burial (just prior to Laramide orogeny)

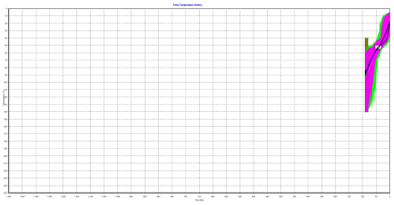

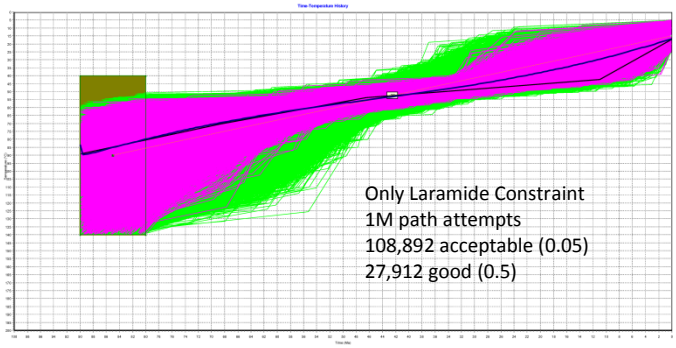
Only Laramide Constraint
1M path attempts
108,892 acceptable (0.05)
27,912 good (0.5)

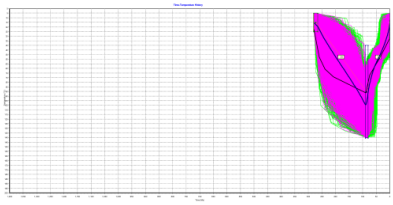

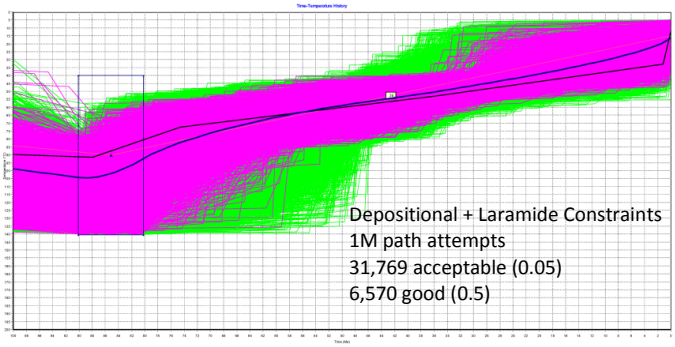
Depositional + Laramide Constraints
1M path attempts
31,769 acceptable (0.05)
6,570 good (0.5)

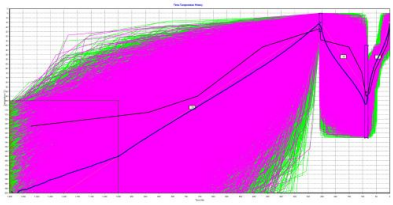

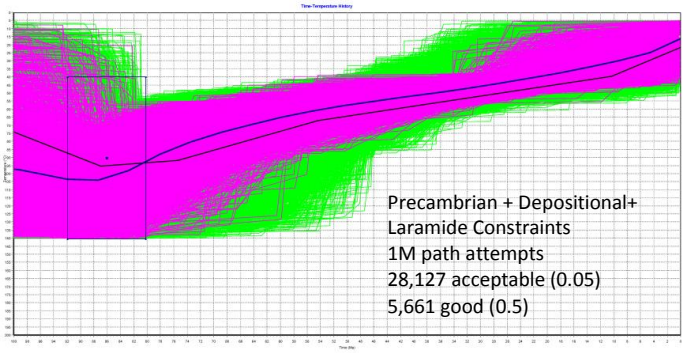
Precambrian + Depositional+
Laramide Constraints
1M path attempts
28,127 acceptable (0.05)
5,661 good (0.5)

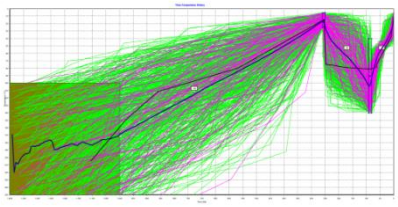

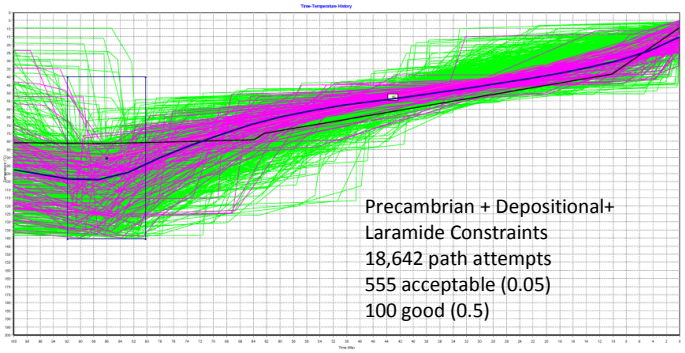
Precambrian + Depositional+
Laramide Constraints
18,642 path attempts
555 acceptable (0.05)
100 good (0.5)

Appendix B: Individual Aliquot results for this study

Sample Number (Table 1)	Sample Name	Radius (μm)	Length (μm)	Width (μm)	Ft	U (ppm)	Th (ppm)	Sm (ppm)	eU	Raw Date (Ma)	Corrected Date (Ma)	1σ error (Ma)
5	K11-VC-2052											
	a3	78.2123	193.68	142.7	0.8156	17.1	20.3	24.2	21.9	58.843	73.4	1.8
6	K11-VC-1790											
	a2	41.6038	111.68	73.8	0.6334	8.9	55.7	12.9	22	18.4622	29.4	0.139
	a3	44.3738	106.03	82.06	0.6584	5	26.4	10.3	11.2	21.8878	33.5	0.261
	a4	41.7314	91.53	79.94	0.6528	50.5	81.4	52.2	69.7	21.3528	32.8	0.227
7	K12-32-SOUTH4											
	a2	69.0909	177.23	124.47	0.7814	4.5	16.1	4.1	8.3	11.8946	15.4	0.143
	a4	44.7753	148.5	74.72	0.6858	30.7	15.8	41.4	34.4	30.103	46.6	0.261
	a5	50.5973	161.24	83.31	0.7138	74.4	100.3	68.8	97.9	24.3852	36	0.367
11	K12-SC1											
	a1	64.2948	176.27	113.31	0.7812	14.2	4.4	15.8	15.2	31.7608	41.5	0.2
	a4	58.4201	190.43	97.92	0.7574	19	10.9	29.1	21.5	16.6697	22.6	0.2
	a5	52.4059	203.7	84.34	0.733	20.3	1.8	7.8	20.8	16.9098	23.9	0.3
12	K12-32-SOUTH7											
	a1	62.906	150.45	116.29	0.7513	22.4	209	30.2	71.5	14.9954	20.2	1
	a2	58.3244	127.52	111.88	0.7379	19.2	102.4	29.7	43.2	17.4294	23.8	0.3

References

Beard, L.S., and Faulds, J.E., 2011, Kingman Uplift, paleovalleys and extensional foundering the northwest Arizona: in Beard, L.S., Karlstrom, K.E., Young, R.A., and Billingsley, G.H., eds., 2011, CREvolution 2—Origin and evolution of the Colorado River system, Workshop Abstracts: U.S. Geological Survey Open-File Report 2011-1210, p. 28-37.

Blackwelder, E., 1934, Origin of the Colorado River: Geological Society of America Bulletin, v. 45, p. 551–566.

Cather, S.M., Chapin, C.E., and Kelley, S. a., 2012, Diachronous episodes of Cenozoic erosion in southwestern North America and their relationship to surface uplift, paleoclimate, paleodrainage, and paleoaltimetry: Geosphere, v. 8, p. 1177–1206, doi: 10.1130/GES00801.1.

Crossey, L.J., Karlstrom, K.E., Springer, a. E., Newell, D.L., Hilton, D.R., and Fischer, T., 2009, Degassing of mantle-derived CO2 and He from springs in the southern Colorado Plateau region--Neotectonic connections and implications for groundwater systems: Geological Society of America Bulletin, v. 121, p. 1034–1053, doi: 10.1130/B26394.1.

Crow, R., Karlstrom, K., Darling, A., Crossey, L., Polyak, V., Granger, D., Asmerom, Y., and Schmandt, B., 2014, Steady incision of Grand Canyon at the million year timeframe: A case for mantle-driven differential uplift: Earth and Planetary Science Letters, v. 397, p. 159–173, doi: 10.1016/j.epsl.2014.04.020.

DeCelles, P., 2004, Late Jurassic to Eocene evolution of the Cordilleran thrust belt and foreland basin system, western USA: American Journal of Science, v. 304, p. 105–168.

Dickinson, W.R., 2012, Rejection of the lake spillover model for initial incision of the Grand Canyon, and discussion of alternatives: Geosphere, v. 9, p. 1–20, doi: 10.1130/GES00839.1.

Dickinson, W.R., and Gehrels, G.E., 2003, U–Pb ages of detrital zircons from Permian and Jurassic eolian sandstones of the Colorado Plateau, USA: paleogeographic implications: Sedimentary Geology, v. 163, p. 29–66, doi: 10.1016/S0037-0738(03)00158-1.

Dickinson, W., Lawton, T., Pecha, M., Davis, S.J., Gehrels, G.E., and Young, R.A., 2012, Provenance of the Paleogene Colton Formation (Uinta Basin) and Cretaceous–Paleogene provenance evolution in the Utah foreland: Evidence from U-Pb ages of: Geosphere, v. 8, p. 854–880, doi: 10.1130/GES00763.1.

Doelling, H., 2008, Geologic map of the Kanab 30’x 60'quadrangle: Kane and Washington counties, Utah, and Coconino …,.

Doelling, H.H., Blackett, R.E., Hamblin, A.H., and Powell, J.D., 2000, Geology of Grand Staircase-Escalante National Monument , Utah:.

Dumitru, T.A., Duddy, I.R., and Green, P.F., 1994, Mesozoic-Cenozoic burial, uplift, and erosion history of the west-central Colorado Plateau: Geology, v. 22, p. 499–502.

Dutton, C.E., 2001, Tertiary history of the Grand Cañon District / Clarence E. Dutton ; with an introduction by Wallace Stegner and a new foreword by Stephen J. Pyne.: Tucson : University of Arizona Press, c2001.

Ehlers, T.A., and Farley, K.A., 2003, Apatite (U–Th)/He thermochronometry: methods and applications to problems in tectonic and surface processes: Earth and Planetary Science Letters, v. 206, p. 1–14.

Farley, K.A., 2000, Helium diffusion from apatite: General behavior as illustrated by Durango fluorapatite: Journal of Geophysical Research: Solid Earth (1978–2012), v. 105, p. 2903–2914.

Farley, K. a., and Stockli, D.F., 2002, (U-Th)/He Dating of Phosphates: Apatite, Monazite, and Xenotime: Reviews in Mineralogy and Geochemistry, v. 48, p. 559–577, doi: 10.2138/rmg.2002.48.15.

Flowers, R.M., 2009, Exploiting radiation damage control on apatite (U–Th)/He dates in cratonic regions: Earth and Planetary Science Letters, v. 277, p. 148–155, doi: 10.1016/j.epsl.2008.10.005.

Flowers, R.M., and Farley, K. a., 2012, Apatite 4He/3He and (U-Th)/He evidence for an ancient Grand Canyon.: Science (New York, N.Y.), v. 338, p. 1616–9, doi: 10.1126/science.1229390.

Flowers, R.M., Shuster, D.L., Wernicke, B., and Farley, K. a., 2007, Radiation damage control on apatite (U-Th)/He dates from the Grand Canyon region, Colorado Plateau: Geology, v. 35, p. 447, doi: 10.1130/G23471A.1.

Flowers, R.M., Wernicke, B., and Farley, K. a., 2008, Unroofing, incision, and uplift history of the southwestern Colorado Plateau from apatite (U-Th)/He thermochronometry: Geological Society of America Bulletin, v. 120, p. 571–587, doi: 10.1130/B26231.1.

Fox, M., and Shuster, D.L., 2014, The influence of burial heating on the (U–Th)/He system in apatite: Grand Canyon case study: Earth and Planetary Science Letters, v. 397, p. 174–183, doi: 10.1016/j.epsl.2014.04.041.

Gehrels, G.E., Blakey, R., Karlstrom, K.E., Timmons, J.M., Dickinson, B., and Pecha, M., 2011, Detrital zircon U-Pb geochronology of Paleozoic strata in the Grand Canyon, Arizona: Lithosphere, v. 3, p. 183–200, doi: 10.1130/L121.1.

Hoffman, M., 2009, Mio-Pliocene erosional exhumation of the central Colorado Plateau, eastern Utah: New insights from apatite (U-Th)/He thermochronometry:.

Karlstrom, K.E., Coblentz, D., Dueker, K., Ouimet, W., Kirby, E., Van Wijk, J., Schmandt, B., Kelley, S., Lazear, G., Crossey, L.J., Crow, R., Aslan, A., Darling, A., Aster, R., et al., 2012, Mantle-driven dynamic uplift of the Rocky Mountains and Colorado Plateau and its surface response: Toward a unified hypothesis: Lithosphere, v. 4, p. 3–22, doi: 10.1130/L150.1.

Karlstrom, K.E., Crow, R., Crossey, L.J., Coblentz, D., and Van Wijk, J.W., 2008, Model for tectonically driven incision of the younger than 6 Ma Grand Canyon: Geology, v. 36, p. 835, doi: 10.1130/G25032A.1.

Karlstrom, K.E., Crow, R.S., Peters, L., McIntosh, W., Raucci, J., Crossey, L.J., Umhoefer, P., and Dunbar, N., 2007, 40Ar/39Ar and field studies of Quaternary basalts in Grand Canyon and model for carving Grand Canyon: Quantifying the interaction of river incision and normal faulting across the western edge of the Colorado Plateau: Geological Society of America Bulletin, v. 119, p. 1283–1312.

Karlstrom, K.E., Lee, J.P., Kelley, S.A., Crow, R.S., Crossey, L.J., Young, R.A., Lazear, G., Beard, L.S., Ricketts, J.W., Fox, M., and Shuster, D.L., 2014a, Formation of the Grand Canyon 5 to 6 million years ago through integration of older palaeocanyons: Nature Geoscience, doi: 10.1038/NGEO2065.

Karlstrom, K.E., Lee, J.P., Kelley, S.A., Crow, R.S., Crossey, L.J., Young, R.A., Lazear, G., Beard, L.S., Ricketts, J.W., Fox, M., and Shuster, D.L., 2014b, Formation of the Grand Canyon 5 to 6 million years ago through integration of older palaeocanyons: Nature geoscience, doi: 10.1038/NGEO2065.

Kelley, S.A., Chapin, C.E., and Karlstrom, K.E., 2001, Laramide Cooling Histories of Grand Canyon, Arizona, and the Front Range, Colorado, Determined from Apatite Fission-track Thermochronology, *in* Young, R.A. and Spamer, E.E. eds., Colorado River: Origin and evolution: Grand Canyon, Arizona, Grand Canyon Association2, Grand Canyon Association, p. 37–46.

Kelley, S.A., and Karlstrom, K.E., 2012, Erosional history of the eastern Grand Canyon : Evidence from apatite fi ssion-track thermochronology: Unpublished, v. 2489, p. 109–117, doi: 10.1130/2012.2489(07).

Ketcham, R. a., 2005, Forward and Inverse Modeling of Low-Temperature Thermochronometry Data: Reviews in Mineralogy and Geochemistry, v. 58, p. 275–314, doi: 10.2138/rmg.2005.58.11.

Lee, J.P., Stockli, D.F., Kelley, S.A., Pederson, J.L., Karlstrom, K.E., and Ehlers, T. a., 2013, New thermochronometric constraints on the Tertiary landscape evolution of the central and eastern Grand Canyon, Arizona: Geosphere, p. 1–13, doi: 10.1130/GES00842.1.

Nations, J., Swift, R., and Jr, H.H., 2000, Summary of Cretaceous stratigraphy and coal distribution, Black Mesa Basin, Arizona: Geologic Assessment of Coal in the Colorado …,.

Pederson, J.L., 2008, The mystery of the pre–Grand Canyon Colorado River—Results from the Muddy Creek Formation: GSA Today, v. 18, p. 4, doi: 10.1130/GSAT01803A.1.

Pederson, J.L., Cragun, W.S., Hidy, a. J., Rittenour, T.M., and Gosse, J.C., 2013, Colorado River chronostratigraphy at Lee's Ferry, Arizona, and the Colorado Plateau bull's-eye of incision: Geology, doi: 10.1130/G34051.1.

Polyak, V., Hill, C., and Asmerom, Y., 2008, Age and evolution of the Grand Canyon revealed by U-Pb dating of water table-type speleothems.: Science (New York, N.Y.), v. 319, p. 1377–80, doi: 10.1126/science.1151248.

Potochnik, A.R., 2001, Paleogeomorphic evolution of the Salt River region: Implications for Cretaceous-Laramide inheritance for ancestral Colorado River drainage: Colorado River: Origin and evolution: Grand Canyon, Arizona, Grand Canyon Association, p. 17–22.

Ranney, W., 2014, A history of ideas on the origin of the the Grand Canyon: Geosphere,.

Shuster, D.L., and Farley, K.A., 2009, The influence of artificial radiation damage and thermal annealing on helium diffusion kinetics in apatite: Geochimica et cosmochimica acta, v. 73, p. 183–196.

Shuster, D.L., Flowers, R.M., and Farley, K.A., 2006, The influence of natural radiation damage on helium diffusion kinetics in apatite: Earth and Planetary Science Letters, v. 249, p. 148–161.

Stockli, D., Farley, K., and Dumitru, T., 2000, Calibration of the apatite (U-Th)/He thermochronometer on an exhumed fault block, White Mountains, California: Geology, doi: 10.1130/0091-7613(2000)28<983.

Timmons, J.M., Karlstrom, K.E., Heizler, M.T., Bowring, S. a., Gehrels, G.E., and Crossey, L.J., 2005, Tectonic inferences from the ca. 1255–1100 Ma Unkar Group and Nankoweap Formation, Grand Canyon: Intracratonic deformation and basin formation during protracted Grenville orogenesis: Geological Society of America Bulletin, v. 117, p. 1573, doi: 10.1130/B25538.1.

Wernicke, B., 2011, The California River and its role in carving Grand Canyon: Geological Society of America Bulletin, v. 123, p. 1288–1316, doi: 10.1130/B30274.1.

Young, R.A., 2001, Geomorphic, structural, and stratigraphic evidence for Laramide uplift of the southwestern Colorado Plateau margin in northwestern Arizona:.

Young, R., and Hartman, J., 2014, Paleogene rim gravel of Arizona: Age and significance of the Music Mountain Formation: Geosphere, p. 870–891, doi: 10.1130/GES00971.1.

Young, R.A., and Spamer, E.E., 2001, The Colorado River: origin and evolution: Grand Canyon Assn.